Automatica 47 (2011) 2571–2583

Contents lists available at SciVerse ScienceDirect

Automatica

journal homepage: www.elsevier.com/locate/automatica

Modelling and control of a flying robot interacting with the environment☆

Lorenzo Marconi, Roberto Naldi [1], Luca Gentili

Center for Research on Complex Automated Systems (CASY) "Giuseppe Evangelisti", DEIS - Department of Electronic, Computer Science and Systems, University of Bologna, Viale Risorgimento 2, 40136 Bologna, Italy

ARTICLE INFO

Article history:
Received 20 February 2009
Received in revised form
6 May 2011
Accepted 16 May 2011
Available online 14 October 2011

Keywords:
UAV
Hybrid automata
Trajectory tracking
Path following
Nonlinear control

ABSTRACT

This work focuses on the problem of modelling and controlling a Ducted-Fan Miniature unmanned Aerial Vehicle (DFMAV) considering explicitly the interaction with the environment and the resulting constraints that affect the system dynamics. The goal is to address a scenario in which DFMAVs accomplish tasks requiring contact between the aerial vehicle and the environment such as remote manipulation, docking and flight in cluttered environments. Since the system's dynamics may be dramatically different when contacts happen and when they do not, an overall description of the system is obtained by collection of the different behaviours into a hybrid automaton. For this particular class of hybrid dynamical systems, a framework for *robust* control of the system based on a path following strategy is developed and tested on a scenario in which the DFMAV is required to dock with and undock from a vertical surface. Simulation results are also presented to show the effectiveness of the proposed framework.

1. Introduction

Recent advances in the design of flight control systems for Unmanned Aerial Vehicles (UAV) have allowed a great variety of civil and military applications to be accomplished by sophisticated autonomous systems (Castillo, Lozano, & Dzul, 2003; Feron & Johnson, 2008; Hughes, 2007; Sullivan, 2006). The effectiveness of UAV in real applications is one of the main reasons for the growing interest in this research field that is often referred to as "aerial robotics". Despite the important results already achieved, the design of control systems for UAV has to face the new challenges posed by future applicative scenarios. Autonomous missions, in fact, more often require vehicle operations next to other vehicles or infrastructure. These operations include, inter alia, take-off and landing –Theodore et al. (2005) – obstacle avoidance – Scherer, Singh, Chamberlain, and Saripalli (2007) – and docking and refuelling –Hansen, Murray, and Campos (2004). These kind of applications are behind the manufacture of miniature VTOL (Vertical Take-Off and Landing) unmanned aircraft, which have shown incredible flight manoeuvrability, as testified for example in Frank, McGrew, Valenti, Levine, and How (2007) and Gavrilets (2003), and seem to have a large potential that has so far been little investigated. The primary reason is probably the fact that the more frequently adopted configuration, the helicopter, has fragile moving blades which should be kept safely away from any rigid obstacle.

A successful VTOL configuration, which overcomes the limitation imposed by the presence of the rotor while at the same time maintaining the manoeuvrability of standard helicopters, is represented by the ducted-fan (Johonson & Turbe, 2005; Naldi, Gentili, Marconi, & Sala, 2010; Pflimlin, Binetti, Trouchet, Soueres, & Hamel, 2007). This class of miniature UAV is characterised by a very simple mechanical structure, composed only of two main subsystems: the propulsive subsystem, composed of a propeller and an electric or endothermic motor, and the attitude control subsystem, composed of a set of profiled actuated flaps. Both the propeller and the flaps are protected by the presence of a cylindrical fuselage, the duct, which can be designed in order to improve the flying qualities Ko, Ohanian, and Gelhausen (2007).

Drawing inspiration from the potential of these VTOL aircraft, the focus of this work is on the modelling and control of miniature aerial vehicles in an innovative scenario in which the interaction with the environment, in terms of desired or even unpredictable contacts, is explicitly considered. The main motivation behind this endeavour is to allow aerial systems to accomplish advanced robotic tasks such as remote manipulation, sample picking, inspections of buildings, etc.

In all the situations in which contacts between the aerial vehicle and the environment occur, the dynamics of the system may dramatically change and the development of a robust control law

☆ This research is framed within the collaborative project AIRobots (Innovative Aerial Service Robots for Remote inspections by contact, ICT 248669) supported by the European Community under the 7th Framework Programme.This paper was not presented at any IFAC meeting. This paper was recommended for publication in revised form by Associate Editor Warren E. Dixon under the direction of Editor Andrew R. Teel.

E-mail addresses: lorenzo.marconi@unibo.it (L. Marconi), roberto.naldi@unibo.it (R. Naldi), l.gentili@unibo.it (L. Gentili).

[1] Tel.: +39 051 2093875; fax: +39 051 209307.

0005-1098/$ – see front matter © 2011 Elsevier Ltd. All rights reserved.
doi:10.1016/j.automatica.2011.09.020

able to handle all the possible interactions becomes a challenge. For this reason we start by investigating the dynamics of the system considering explicitly the possible constraints deriving from the interaction with the environment and, drawing inspiration from recent advances in robotics –Egerstedt (2000) – manoeuvre-based control –Frazzoli, Dahleh, and Feron (2005) and Sanfelice and Frazzoli (2008) – and hybrid control systems theory –Goebel, Sanfelice, and Teel (2009) and Matveev and Savkin (2000) – we collect a set of different lower complexity dynamical models, each one describing only a particular flight condition, to form a hybrid automaton, Lygeros, Johansson, Simić, Zhang, and Sastry (2003) and Tavernini (1987).

With the hybrid automaton in hand, in the second part of the paper we develop a control framework to govern the DFMAV in presence of uncertainties. The developed control framework rests upon a *path following* strategy, Skjetne, Fossen, and Kokotovic (2004), in which the reference trajectory used for control purposes is characterised by a *geometric path* parametrised by a *time law*. The resulting control architecture is constituted by a set of low level controllers, associated to the specific operative modes of the vehicle, and a supervisor properly enabling the low level controller and setting the appropriate time law according to the actual operative mode and state of the vehicle and to the desired task. The control architecture is tested on a manoeuvre in which the vehicle is required to dock with a vertical surface starting from a free-flight configuration, to slide along it by tracking a desired state reference signal, and, finally, to undock from the vertical surface by reaching again a free-flight configuration. Simulation results are presented to show the effectiveness of the proposed framework.

The manuscript is organised as follows. Section 2 presents the dynamics of the miniature aerial vehicle of interest for this paper and the interaction scenario. Section 3 discusses the framework for the control of the DFMAV with special emphasis towards the docking–undocking test manoeuvre. Simulation results are shown in Section 4. Finally, Section 5 concludes with final remarks.

Notations.

$\mathbb{R}$ and $\mathbb{R}_+$ denote respectively the field of real and positive real numbers. For $x \in \mathbb{R}^n$, $|x|$ denotes the Euclidean norm and, for $\mathcal{A}$ a closed subset of $\mathbb{R}^n$, $|x|_{\mathcal{A}} = \min_{y\in\mathcal{A}} |x - y|$ denotes the distance of x from $\mathcal{A}$. For a bounded function $f : \mathcal{D} \to \mathbb{R}^n$, $\mathcal{D} \subset \mathbb{R}$, $\|f\|_\infty$ denotes the infinity norm defined as $\sup_{t\in\mathcal{D}} |f(t)|$. For a vector $x \in \mathbb{R}^n$, the notation $\mathcal{B}_\mu(x)$ denotes the n-dimensional ball of radius μ with centre in x. For a closed set $\mathcal{A} \subset \mathbb{R}^n$ and a positive integer μ, the notation $\mathcal{A}+\mathcal{B}_\mu$ denotes the set $\{x \in \mathbb{R}^n : |x|_{\mathcal{A}} \leq \mu\}$. The notation $f : \mathcal{D} \rightrightarrows \mathcal{C}$ denotes a set-valued map.

2. DFMAV modelling and interaction scenario

We focus on a miniature ducted-fan configuration, sketched in Fig. 1, composed of a fixed pitch propeller (without collective/cyclic pitches and tail rotor as in the helicopter) and of a number of actuated flaps positioned below the propeller that deviate the air flow in order to generate anti-torque and the forces/torques needed to gain full controllability, Johonson and Turbe (2005), Marconi and Naldi (2006) and Pflimlin et al. (2007). The system has all the degrees-of-freedom of a helicopter but with a very simple and reliable mechanical structure. Furthermore, the shroud allows the vehicle to safely interact with the environment avoiding dangerous collisions between the moving blades and obstacles. For the sake of simplicity, we limit the analysis only to the "planar dynamics" on the configuration manifold $S_1 \times \mathbb{R}^2$ (see Fig. 1). The general "spatial dynamics", defined on the configuration manifold $SO(3)\times\mathbb{R}^3$, can be dealt with in a similar, though heavier, way from a notational viewpoint.

We consider the DFMAV in the two possible flight modes denoted as "free flight" and "vertical interaction" (see Fig. 1), with the latter representative of a possible scenario in which the vehicle slides in contact with the environment in order to perform robotic tasks (such as sample picking, data collection by contact, grasping, etc.). Specifically, we address the control task in which the vehicle is required to dock with and to undock from the vertical surface. In this respect the DFMAV is considered as a rigid body which may come into contact with rigid surfaces through the contact points P_{V1} and P_{V2} (see Fig. 1). From a technological viewpoint, it is also assumed that the points P_{V1} and P_{V2} are equipped with contact sensors (such as force or tactile sensors, Nicholls & Lee, 1989), so that the specific operative mode in which the DFMAV operates is known.

2.1. Force/torque generation mechanism

To model forces and torques generation mechanism, standard aerodynamic arguments are considered Stengel (2004) by assuming the system in almost stationary flight and by neglecting all possible aerodynamic forces caused by the forward speed of the system except for the aerodynamic resistance, Johonson and Turbe (2005), Ko et al. (2007) and Pflimlin et al. (2007).

Each flap is modelled as a wing with area S_{flap} immersed into a relative wind velocity denoted as V_e, so that the aerodynamic lift force is approximated by $F = 0.5\rho S_{\text{flap}} C_L V_e^2$, where ρ is the air density and C_L is the lift coefficient. By assuming airfoil profiles with small Reynolds numbers and with reasonably small angles of attack, the lift coefficient can be approximated by $C_L = a_F u_F$, with a_F a constant coefficient that depends on the geometry of the flap, and where u_F, the angle of attack with respect to the propeller downwash, represents the control input used to manipulate the flap's force. Drag forces are neglected by assuming an aerodynamically efficient flap subsystem.

The flap's relative wind velocity V_e is assumed equal to the output velocity of the air generated by the rotor given by $V_e = \sqrt{u_M/(2\rho S_{\text{disk}})}$ in which u_M is the propeller thrust and S_{disk} denotes the area of the propeller disk. Hence, the expression of the flap lift F can be rewritten as $F = k_F u_F u_M$ where $k_F = a_F S_{\text{flap}}/S_{\text{disk}}$. It is assumed that u_M and u_F are the available control inputs whose amplitude is limited by physical constraints. In particular, the propeller thrust, which can be applied in one direction and it is limited by the maximum power characterizing the electric motor, ranges in the set $u_M \in [\underline{u}_M, \bar{u}_M]$, with $0 < \underline{u}_M \leq \bar{u}_M$ and $\bar{u}_M$ greater than the gravity force, while u_F, because of mechanical and aerodynamical limitation, ranges in the set $u_F \in [-\bar{u}_F, \bar{u}_F]$, with $\bar{u}_F$ a given positive number.

2.2. Free flight model

The Newton–Euler equations of motion of a rigid body in the configuration manifold $S_1 \times \mathbb{R}^2$ are used to model the free flight mode, Naldi et al. (2010). With $F_i = \{O_i, \vec{i}_i, \vec{j}_i\}$ and $F_b = \{O_b, \vec{i}_b, \vec{j}_b\}$ respectively an inertial and body coordinate frame fixed in the centre of mass of the aircraft, and with $\theta \in \mathbb{R}$ the angle parametrising the S_1 manifold (see Fig. 1), the position $\text{col}(x, z)$ of the centre of mass in F_i is governed by the differential equations

$$\begin{aligned} M\ddot{x} &= u_M \sin\theta + k_F u_M u_F \cos\theta - F^x_{\text{drag}} \\ M\ddot{z} &= u_M \cos\theta - k_F u_M u_F \sin\theta - Mg - F^z_{\text{drag}} \\ J\ddot{\theta} &= -k_\tau u_M u_F \end{aligned} \tag{1}$$

in which M and J are respectively the vehicle mass and inertia, $k_\tau = d a_F S_{\text{flap}}/S_{\text{disk}}$, with d the lever arm of the flap's force with respect to the centre of mass of the vehicle, and F^x_{drag} and F^z_{drag} model the aerodynamic drag forces along the longitudinal and vertical direction.

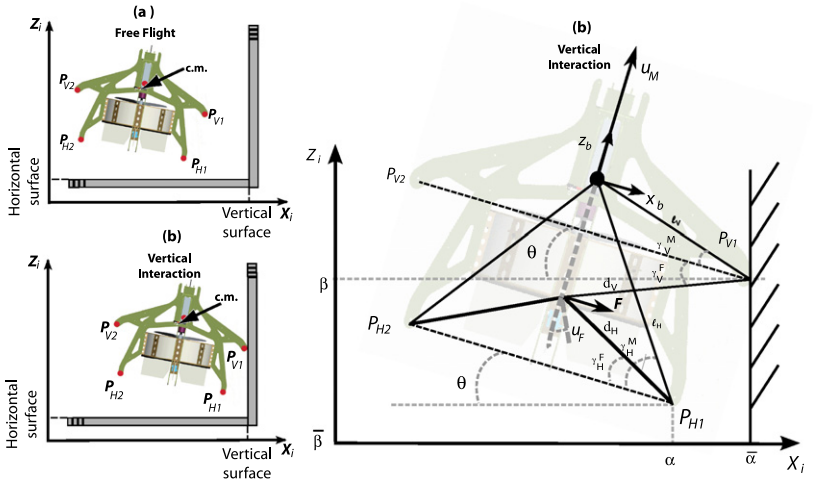

Fig. 1. The two operative modes considered in this paper, namely free-flight (a) and vertical interaction (b) on the configuration manifold $S_1 \times \mathbb{R}^2$.

Motivated by the fact that the value of $k_F \bar{u}_F$ is very small, the model (1) can be simplified by neglecting the body forces $k_F u_M u_F \cos\theta$ and $k_F u_M u_F \sin\theta$ acting on the $\ddot{x}$ and $\ddot{z}$ dynamics (see also Hauser, Sastry, & Meyer, 1992). Moreover, by following the analysis in Ko et al. (2007) and Pflimlin et al. (2007) that shows how, at moderate speed, the most relevant drag effect is represented by the so-called *ram-drag*, we obtain $F^x_{\text{drag}} \approx \lambda_x \dot{x}$ and $F^z_{\text{drag}} \approx 0$, with λ_x a constant coefficient. The free-flight dynamics is then rewritten as

$$\begin{aligned} M\ddot{x} &= u_M \sin\theta - \lambda_x \dot{x} \\ M\ddot{z} &= u_M \cos\theta - Mg \\ J\ddot{\theta} &= -k_\tau u_M u_F. \end{aligned} \tag{2}$$

While the simplified model (2) is used for control design purposes, (1) is used in simulation to test the effectiveness of the proposed solution.

2.2.1. Interaction with a vertical fixed surface

In this section we model the system in the "vertical interaction" scenario in which the UAV slides along a vertical surface by possibly rotating around the pivot P_{V1} (see Fig. 1). For the sake of simplicity, we just consider the cases in which the impact takes place with a vertical (i.e. oriented along the Z_i axis) surface located on the right side of the vehicle at $x = \bar{\alpha}$. More complicated scenarios involving the interaction with shaped surfaces can be treated by properly adapting the forthcoming analysis. This operative mode may be representative of situations in which the UAV is required to accomplish specific tasks by interaction, such as data acquisition by contact or others robotic tasks.

Denoting by $\beta = z - \ell_V \sin(\theta + \gamma_V^M)$ the position of P_{V1} along the Z_i axis, the generalised forces $\mathcal{F}_\theta(u_M, u_F)$ and $\mathcal{F}_\beta(z, \dot{z}, \theta, \dot{\theta}, u_M, u_F)$ acting on the vehicle with respect to the generalised coordinates θ and β are given by

$$\begin{pmatrix} \mathcal{F}_\theta \\ \mathcal{F}_\beta \end{pmatrix} = G(\theta) \begin{pmatrix} u_M \\ u_M u_F \end{pmatrix} - \Lambda \dot{\beta} \tag{3}$$

in which

$$G(\theta) := \begin{pmatrix} \ell_V \cos\gamma_V^M & -k_F d_V \sin\gamma_V^F \\ \cos\theta & -k_F \sin\theta \end{pmatrix} \qquad \Lambda = \begin{pmatrix} 0 \\ \lambda_V \end{pmatrix} \tag{4}$$

where λ_V is the viscous friction of the vertical surface, and γ_V^M and γ_V^F are the angles between the body axis X_b and the arm of lengths ℓ_V and, respectively, d_V in Fig. 1. We observe that the matrix $G(\theta)$ in (4) is invertible for any θ satisfying

$$-\gamma_V^M < \theta < \gamma_V^F. \tag{5}$$

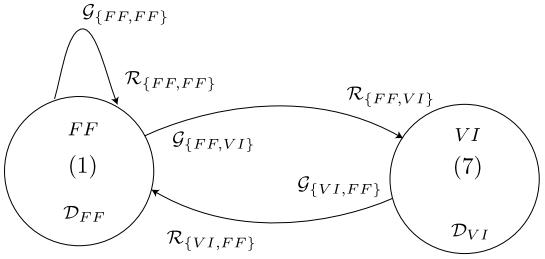

Fig. 2. The hybrid automaton referring to the restricted interaction scenario considered in the paper.

The Lagrangian function of the system, by considering kinetic and potential energies, can be computed as

$$\begin{aligned} \mathcal{L} = {} & \frac{1}{2} M \left(\dot{\beta} + 2\ell_V \cos(\theta + \gamma_V^M)\dot{\beta}\dot{\theta} + \ell_V^2 \dot{\theta}^2 \right) \\ & - Mg \left(\beta + \ell_V \sin(\theta + \gamma_V^M) \right) \end{aligned} \tag{6}$$

and it is governed by the Lagrangian equations

$$\frac{d}{dt}\frac{\partial \mathcal{L}}{\partial \dot{\beta}} - \frac{\partial \mathcal{L}}{\partial \alpha} = \mathcal{F}_\beta, \qquad \frac{d}{dt}\frac{\partial \mathcal{L}}{\partial \dot{\theta}} - \frac{\partial \mathcal{L}}{\partial \theta} = \mathcal{F}_\theta,$$

which, after simple computations, yield

$$\begin{aligned} & M\left(\ddot{\beta} + \ell_V \cos(\theta + \gamma_V^M)\ddot{\theta} - \ell_V \sin(\theta + \gamma_V^M)\dot{\theta}^2 + g \right) \\ & \quad = \mathcal{F}_\beta(z, \dot{z}, \theta, \dot{\theta}, u_M, u_F), \\ & M\left(\ell_V \ddot{\beta} \cos(\theta + \gamma_V^M) + \ell_V^2 \ddot{\theta} + g\ell_V \cos(\theta + \gamma_V^M) \right) \\ & = \mathcal{F}_\theta(u_M, u_F). \end{aligned} \tag{7}$$

This is a 4-th order system with state $(\beta, \dot{\beta}, \theta, \dot{\theta})$ (or, alternatively, by the definition of β, with state $\text{col}(z, \dot{z}, \theta, \dot{\theta})$), and inputs u_M and u_F. In this operative mode, the lateral coordinate x is constrained to be $x = \bar{\alpha} - \ell_V \cos(\theta + \gamma_V^M)$.

For control purposes, it is worth developing the model (7) by introducing two new "virtual" control inputs $\mathcal{F}_1$ and $\mathcal{F}_2$ defined, in terms of the generalised forces $\mathcal{F}_\theta$, $\mathcal{F}_\beta$, as

$$\begin{pmatrix} \mathcal{F}_1 \\ \mathcal{F}_2 \end{pmatrix} = L(\theta)^{-1} \left(\begin{pmatrix} \mathcal{F}_\theta \\ \mathcal{F}_\beta \end{pmatrix} + \Lambda \dot{\beta} \right) \tag{8}$$

in which

$$L(\theta) := M \begin{pmatrix} \ell_V^2 & \ell_V \cos(\theta + \gamma_V^M) \\ \ell_V \cos(\theta + \gamma_V^M) & 1 \end{pmatrix}$$

and Λ is defined as in (4). In terms of the new inputs $\mathcal{F}_1$ and $\mathcal{F}_2$ the dynamics (7) read as

$$\ddot{\theta} = \mathcal{F}_1 - \ell_\theta(\theta, \dot{\theta}, \dot{\beta}, \lambda_V) \qquad \ddot{\beta} = \mathcal{F}_2 - \ell_\beta(\theta, \dot{\theta}, \dot{\beta}, \lambda_V) \tag{9}$$

where

$$\ell_\theta(\theta, \dot{\theta}, \dot{\beta}, \lambda_V) := \frac{\cos(\theta + \gamma_V^M)\dot{\theta}^2}{\sin(\theta + \gamma_V^M)} - \frac{\lambda_V \dot{\beta} \cos(\theta + \gamma_V^M)}{M \ell_V \sin^2(\theta + \gamma_V^M)}$$

$$\ell_\beta(\theta, \dot{\theta}, \dot{\beta}, \lambda_V) := g - \frac{\ell_V \dot{\theta}^2}{\sin(\theta + \gamma_V^M)} + \frac{\lambda_V \dot{\beta}}{M \sin^2(\theta + \gamma_V^M)}.$$

In the subsequent sections we use, for control purposes, the model (9) instead of (7). In this respect, by (3) and by invertibility of $G(\theta)$ for all θ satisfying (5), the relation between the "virtual" inputs $(\mathcal{F}_1, \mathcal{F}_2)$ and the "real" inputs (u_M, u_F) is given by

$$\begin{pmatrix} u_M \\ u_M u_F \end{pmatrix} = G^{-1}(\theta) L(\theta) \begin{pmatrix} \mathcal{F}_1 \\ \mathcal{F}_2 \end{pmatrix} \tag{10}$$

for all θ such that (5) holds. Hence, with $u_M \in [\underline{u}_M, \bar{u}_M]$, $\underline{u}_M > 0$, the real inputs (u_M, u_F) can be always retrieved from the virtual inputs $(\mathcal{F}_1, \mathcal{F}_2)$ provided that θ satisfies (5). Furthermore, we regard the viscous friction λ_V as uncertain with a nominal value denoted by λ_{V0}.

2.3. A hybrid dynamical model of the overall dynamics

A description of the overall dynamics is obtained by means of a *hybrid automaton* (see Goebel et al., 2009), whose hybrid states correspond to the possible operative modes described above (see Fig. 2). In this part we briefly review the definition of hybrid automaton by focusing on the UAV framework. The hybrid automaton captures also un-ideal situations characterizing realistic flight conditions, such as undesired "rebounds" that the UAV might undergo in the manoeuvre of docking with a vertical surface starting from a free-flight configuration.

For notational convenience, let

$$\xi = \begin{pmatrix} x & \dot{x} & z & \dot{z} & \theta & \dot{\theta} \end{pmatrix}^T \quad \text{and} \quad u = \begin{pmatrix} u_M & u_F \end{pmatrix}^T$$

the state and the inputs of the considered system and by U the set in which the control inputs are allowed to range, i.e. $U = [\underline{u}_M, \bar{u}_M] \times [-\bar{u}_F, \bar{u}_F]$. Then a hybrid automaton is identified by the following objects:

- A *set of operative modes* Q which, in the framework addressed in the paper, is given by two modes denoted by $Q = \{FF, VI\}$ with the following meanings:
  - FF, *Free Flight*. None of the points P_{Hi} and P_{Vi}, $i = 1, 2$, are in contact with the environment;
  - VI, *Vertical Interaction*. The point P_{V1} (or, alternatively, P_{V2}) is in contact with the vertical surface.
- A *domain mapping* $\mathcal{D} : Q \rightrightarrows \mathbb{R}^6 \times \mathbb{R}^2$ that defines, for any $q \in Q$, the set of whole state and input space where the continuous variable ξ and control input u may range in the specific operative mode. The domain state and input space is assumed to be a Cartesian product denoted by $\mathcal{D}(q) = \mathcal{D}_\xi(q) \times \mathcal{D}_u(q)$. By the analysis in the previous subsections, the domain mapping, for the operative modes FF and VI, is defined in the following way:
  - $\mathcal{D}(FF) = \mathbb{R}^6 \times U$;
  - $\mathcal{D}(VI) = \mathcal{D}_\xi(VI) \times U$ with $\mathcal{D}_\xi(VI) = \{\xi \in \mathbb{R}^6 : x + \ell_V \cos(\theta + \gamma_V^M) \geq \bar{\alpha}_L\}$, with $\bar{\alpha}_L$ the lower bound of the position $\bar{\alpha}$, i.e. $\bar{\alpha} > \bar{\alpha}_L$.
- A locally Lipschitz *flow map* $f : Q \times \mathbb{R}^6 \times \mathbb{R}^2 \to \mathbb{R}^6$ which describes the continuous evolution of the dynamics while a specific operative mode is active. For every $q \in Q$, the flow map is only defined on $\mathcal{D}(q)$. In our framework, according to Section 2, the flow maps are specified as follows:
  - $f(FF, \xi, u)$, defined for $(\xi, u) \in \mathcal{D}(FF)$, is given by the 6-th order dynamics (2);
  - $f(VI, \xi, u)$, defined for $(\xi, u) \in \mathcal{D}(VI)$, is given by the 4-th order dynamics (7).
- A *set of edges* $\mathcal{E} \subset Q \times Q$ that identifies pairs (q_1, q_2) such that the transition from the operative mode q_1 to q_2 is possible under certain conditions. In our simplified framework the two pairs $\{FF, VI\}$ and $\{VI, FF\}$ belong to $\mathcal{E}$. Furthermore, in order to model realistic cases in which the impact with the vertical surface is *impulsive* but non-completely inelastic, and thus the UAV might undergo "rebounds" while docking, a "self-loop" in the hybrid state FF is also considered. Hence, also the edge $\{FF, FF\}$ belongs to $\mathcal{E}$.
- A *guard mapping* $\mathcal{G} : \mathcal{E} \rightrightarrows \mathbb{R}^6 \times \mathbb{R}^2$ that, for each $(q_1, q_2) \in \mathcal{E}$, identifies the set $\mathcal{G}(q_1, q_2)$ to which the continuous state ξ and the control inputs u have to belong for the transition from q_1 to q_2 to be enabled.
  A special role in the computation of $\mathcal{G}(\{FF, VI\})$, $\mathcal{G}(\{VI, FF\})$ and $\mathcal{G}(\{FF, FF\})$ is played by

$$F_X(\theta, u_M, u_F) = u_M \sin\theta + k_F u_M u_F \cos\theta \tag{11}$$

that represents the resultant force acting on the vehicle along the X_i axis, and by $\alpha_V(x, \theta) := x + \ell_V \cos(\theta + \gamma_V^M)$ that denotes the horizontal position of the contact point P_{V1}. Furthermore, according to the impact theory of rigid bodies (see Brogliato, 1996), possible rebounds can be characterised in terms of the value of the so-called *coefficient of restitution* c_R along the lateral direction. The latter is a dimensionless coefficient relating the lateral velocity $\dot{\alpha}_V$ of the contact point P_{V1} before and after the impact. It takes value in the interval [0, 1], with $c_R = 0$ and $c_R = 1$ modelling a totally inelastic and elastic impact, respectively. The value of the coefficient depends on a number of mechanical features of the impacting bodies (such as viscoelastic properties of the materials and plastic deformation and geometry of the contact surfaces, see Goldsmith, 1960), and its structural properties are affected by the value of F_X and $\dot{\alpha}_V$ at the impact, i.e. $c_R(F_X, \dot{\alpha}_V)$. Large forces and small speed at the impact typically result into inelastic impacts (i.e. $c_R = 0$) and thus absence of rebounds. On the contrary, small lateral forces and large lateral speed result in elastic impacts with the exact value of $c_R \in (0, 1]$ dependent on mechanical properties of the impacting materials. The dependence of c_R on $(F_X, \dot{\alpha}_V)$ can be obtained by considering a damped compliant impact model (see Brogliato, 1996). Specifically, denoting by ν the lateral deformation of the impacting material, it is assumed that, in the small interval of time δT_i in which the impact dynamics take place, the deformation is governed by the linear differential equation

$$M(\ddot{\nu} + k_d \dot{\nu} + k_e \nu) = F_X(\theta, u_M, u_F) \tag{12}$$

where k_d and k_e denote the dissipative and elastic coefficients of the material, respectively. The initial conditions of the previous dynamics at the impact time t_i are $(\nu(t_i), \dot{\nu}(t_i)) = (0, \dot{\alpha}_V(t_i))$. By assuming $F_X(t) \equiv F_X(t_i) = \text{const}$, for $t \in [t_i, t_i + \delta T_i]$ (assumption motivated by the negligible duration of the impact interval in relation to the time constants of the vehicle state and input variables), the impact can be considered inelastic (i.e. $c_R = 0$) if $\nu(t) \geq 0$ for all $t \in t_i + \delta T_i$, and elastic otherwise. In the latter case $c_R = \bar{c}_R$ with $\bar{c}_R \in (0, 1]$ dependent on the properties of the impacting material.

With these functions at hand, the guard mappings involving *FF* and *VI* are naturally defined as follow:

- $\mathcal{G}(\{FF, VI\}) = \{(\xi, u) \in \mathcal{D}(FF)\colon F_X(\theta, u_M, u_F) \geq 0, \alpha_V(x, \theta) \geq \bar{\alpha}, c_R(F_X, \dot{\alpha}_V) = 0\}$;
- $\mathcal{G}(\{FF, FF\}) = \{(\xi, u) \in \mathcal{D}(FF)\colon F_X(\theta, u_M, u_F) \geq 0, \alpha_V 0xub(x, \theta) \geq \bar{\alpha}, c_R(F_X, \dot{\alpha}_V) > 0\}$;
- $\mathcal{G}(\{VI, FF\}) = \{(\xi, u) \in \mathcal{D}(VI)\colon F_X(\theta, u_M, u_F) < 0\}$.

- A *reset map* $\mathcal{R} : \mathcal{E} \times \mathbb{R}^6 \times \mathbb{R}^2 \to \mathbb{R}^6$ that, for each $(q_1, q_2) \in \mathcal{E}$ and $(\xi, u) \in \mathcal{G}(q_1, q_2)$, identifies the jump of the state variable during the transition from q_1 to q_2. The reset maps of interest can be specified as follows:
  - $\mathcal{R}(\{FF, VI\}, (\xi, u))$ can be computed under the inelastic impact assumption discussed above and by energy conservation arguments. For the sake of simplicity we assume that the impact takes place with zero vertical speed, i.e. $\dot{z} = 0$ at the impact time. Let $(\dot{x}^-, \dot{\theta}^-)$ and $(\dot{x}^+, \dot{\theta}^+)$ be the lateral and angular velocity just before and after the impact, respectively. The kinetic energy of the vehicle before and after the impact can be computed respectively as $E^- = M(\dot{x}^-)^2/2 + J(\dot{\theta}^-)^2/2$ and $E^+ = M\ell_V(\dot{\theta}^+)^2/2$. The latter, in view of the inelastic impact assumption, has been computed by modelling the UAV as a pendulum constrained at P_{V1} with mass M and length ℓ_V. With $c_E \in (0, 1]$ an energy loss coefficient (modelling the energy loss due to plastic deformation of the material, see Brogliato, 1996), we have $(E^+)^2 = c_E(E^-)^2$ by which $\dot{\theta}^+ = c_E((\dot{x}^-/\ell_V)^2 + (J/M)(\dot{\theta}^-/\ell_V)^2)^{1/2}$. Then, by considering the expression of $\mathcal{D}(VI)$, $\dot{x}^+ = \ell_V \sin(\theta + \gamma_V^M)\dot{\theta}^+$. Overall, the map $\mathcal{R}(\{FF, VI\}, (\xi, u))$ is thus a function that associates to $(\xi, u) \in \mathcal{D}(FF)$ the element
$$\xi' = \mathrm{col}\left(x, c_E\ell_V \sin(\theta + \gamma_V^M)\sqrt{\frac{\dot{x}^2}{\ell_V^2} + \frac{J\dot{\theta}^2}{M\ell_V^2}}, z, \dot{z}, \theta, c_E\sqrt{\frac{\dot{x}^2}{\ell_V^2} + \frac{J\dot{\theta}^2}{M\ell_V^2}}\right).$$
  - We derive now $\mathcal{R}(\{FF, FF\}, (\xi, u))$ by assuming, as above, that $\dot{z} = 0$ at the impact time. The reset relation for $\dot{\theta}$ is obtained by the same energy conservation arguments used before for $\mathcal{R}(\{FF, VI\}, (\xi, u))$, by assuming that, at the impact, the vehicle undergoes an instantaneous angular acceleration while pivoting around the contact point P_{V1}. It turns out that $\dot{\theta}^+ = c_E((\dot{x}^-/\ell_V)^2 + (J/M)(\dot{\theta}^-/\ell_V)^2)^{1/2}$. As far as the reset relation for $\dot{x}$ is concerned, the arguments above cannot be used any more as α_V is not constrained after the impact. Rather, by the definition of c_R, the lateral velocity $\dot{\alpha}_V$ of P_{V1} before and after the impact satisfies $\dot{\alpha}_V^+ = -c_R(F_X(\theta^-, u_M^-, u_F^-), \dot{\alpha}_V^-)\,\dot{\alpha}_V^-$ with obvious meaning of the acmes "−" and "+". By this and the definition of α_V it follows that $\dot{x}^+ = \ell_V \sin(\theta^+ + \gamma_V^M)\,\dot{\theta}^+ - c_R(F_X(\theta^-, u_M^-, u_F^-), \dot{\alpha}_V^-)\,\dot{\alpha}_V^-$. Thus, using the fact that $\theta^+ = \theta^-$ (instantaneous impact), the map $\mathcal{R}(\{FF, FF\}, (\xi, u))$ is a function that associates to $(\xi, u) \in \mathcal{D}(FF)$ the element
$$\xi' = \mathrm{col}\left(x, \ell_V\, c_E\, \sin(\theta + \gamma_V^M)\sqrt{\frac{\dot{x}^2}{\ell_V^2} + \frac{J\dot{\theta}^2}{M\ell_V^2}} - c_R\dot{\alpha}_V,\ z,\ \dot{z},\ \theta, c_E\sqrt{\frac{\dot{x}^2}{\ell_V^2} + \frac{J\dot{\theta}^2}{M\ell_V^2}}\right)$$
with $c_R = c_R(F_X(\theta, u_M, u_F), \dot{\alpha}_V)$. In the previous model it is clearly assumed that value of c_E is such that the overall kinetic energy of the vehicle after the impact is lower or equal to the one before the contact.
  - Finally, $\mathcal{R}(\{VI, FF\}, (\xi, u))$ is simply the identity, namely $\mathcal{R}(\{VI, FF\}, (\xi, u)) = \xi$.

3. DFMAV control over desired manoeuvres

With the hybrid automaton in hand, a few results regarding the control of the aerial vehicle in order to execute desired manoeuvres are now presented. For compactness, attention is focused on a specific test manoeuvre in which the aerial vehicle, starting from a free-flight mode, is required to dock with a vertical surface, to slide along it by tracking a desired state reference signal, and, finally, to undock from the vertical surface by reaching again a free-flight configuration (see Fig. 4).

The control architecture rests upon a *path following* strategy, in which the reference trajectory used to design the control law is characterised by a *geometric path* parametrised by a variable usually referred to as the *time law*. Path following was already shown to be a successful strategy in several control fields, such as robotics Coelho and Nunes (2005), aerospace Scharf, Ploen, and Hadaegh (2003), underwater vehicles Antonelli, Fossen, and Yoerger (2008). It is also effective in handling robustness issues, Aguiar, Hespanha, and Kokotovic (2005) and Skjetne et al. (2004).

The resulting control architecture is constituted by a set of low level controllers, associated to the specific operative modes in which the vehicle operates (FF and VI for the considered test manoeuvre), and a supervisor. The role of the latter is to enable the appropriate low level controller and a time law strategy according to the actual state and operative mode of the vehicle and to the desired task.

A preliminary step in the design of the control law consists of the computation of state and input reference trajectories according to the path following strategy. This is done in the next subsection. Then, in the subsequent two subsections, the low level control synthesis and the design of the supervisor are addressed.

3.1. Reference manoeuvres

With $\varrho : \mathbb{R} \to \mathbb{R}$ a smooth function and $\mathfrak{q}(t) := (\varrho(t)\ \dot{\varrho}(t)\ \cdots\ \varrho^{(s-1)}(t))$, $s > 0$, a reference manoeuvre for the system in the operative mode $q \in Q$ is given by a smooth function $\xi^\star(\mathfrak{q}(t)) \in \mathcal{D}(q)$, denoted as state manoeuvre, and a bounded function $u^\star(\mathfrak{q}(t)) \in U$, denoted as an input manoeuvre, satisfying
$$\frac{d\xi^\star(\mathfrak{q}(t))}{d\mathfrak{q}}\dot{\mathfrak{q}}(t) = f(q, \xi^\star(\mathfrak{q}(t)), u^\star(\mathfrak{q}(t))) \tag{13}$$
for almost all t and for some $s > 0$. We refer to the vector $\mathfrak{q}(t)$ and to the set $\mathrm{gr}\,(\xi^\star, u^\star)|_\Sigma := \{(\xi', u') \in \mathcal{D}(q) : (\xi', u') = (\xi^\star(\mathfrak{q}), u^\star(\mathfrak{q})), \mathfrak{q} \in \Sigma\}$ respectively as the time law and the geometric-path of the manoeuvre. In the previous definition $\Sigma \subset \mathbb{R}^s$ is the set where the time law is supposed to range while s is a positive number related to the relative degree of the system. Reference manoeuvres can be obtained by nominal inversion of the system dynamics as detailed in Appendix A for the operative modes FF and VI.

Due to the presence of possible parametric/dynamic uncertainties, exogenous disturbances and others un-ideal initial conditions that make the controlled plant behaving differently from desired manoeuvres, a crucial step is to generate *robust reference manoeuvres* whose practical (and not perfect) tracking does not generate unwanted switches between operative modes in the actual motion of the plant. In the following, robustness is quantified by means of a positive parameter μ that, roughly, quantify how far the actual motion of the plant can be with respect to the reference manoeuvre in order to avoid unplanned changes of operative modes and to effectively switch to the desired operative mode. With reference to the docking–undocking test manoeuvre, robust reference manoeuvres of interest can be characterised as follows:

- *a. Docking reference manoeuvre.* This is the first manoeuvre designed to have the vehicle approaching the vertical surface starting from a free-flight configuration. Mathematically, the

reference manoeuvre is a smooth function $\xi_a^\star(\mathfrak{q}(t)) \in \mathcal{D}(FF)$ and a bounded function $u_a^\star(\mathfrak{q}(t)) \in U$ of the form specified in Appendix A, where $\mathfrak{q}(t) \subset \mathbb{R}^5$ is the specific time law. The latter is supposed to range in the set $\Sigma_a \subset \mathbb{R}^5$ to be properly designed, along with the geometric-path, so that the reference manoeuvre lends itself to design control laws effective in enforcing the desired docking manoeuvre. Specifically, it is supposed that there exist Σ_a', $\Sigma_a'' \subset \Sigma_a$ such that the following properties hold:

$$\begin{aligned}
&(\mathrm{gr}(\xi_a^\star, u_a^\star)|_{\Sigma_a} + \mathcal{B}_\mu) \bigcap \left(\bigcup_{\{FF,q\}\in\mathcal{E}\setminus\{FF,VI\}} \mathcal{G}(\{FF,q\}) \right) = \emptyset;\\
&(\mathrm{gr}(\xi_a^\star, u_a^\star)|_{\Sigma_a'} + \mathcal{B}_\mu) \bigcap \left(\bigcup_{\{FF,q\}\in\mathcal{E}} \mathcal{G}(\{FF,q\}) \right) = \emptyset;\\
&(\mathrm{gr}(\xi_a^\star, u_a^\star)|_{\Sigma_a''} + \mathcal{B}_\mu) \subset \mathcal{G}(\{FF,VI\}).
\end{aligned} \tag{14}$$

The first condition simply asks, in geometric terms, that the reference manoeuvre lies at least μ-distant from all the guard sets that, if intersected, would enable a switch to a different undesired (i.e. different from VI) operative mode. This guarantees that each state and input trajectory evolving μ-close to the reference manoeuvre is possibly subject to a switch to the mode VI only. On the other hand, the second condition requires that, as long as $\mathfrak{q}(t) \in \Sigma_a'$, any manoeuvre taking place μ-close to the reference is guaranteed to remain in the FF mode. Finally, the last condition ensures that for each $\mathfrak{q}(t) \in \Sigma_a''$, any state and input trajectories μ-close to the reference is necessarily inside $\mathcal{G}(\{FF,VI\})$. Thus, under the assumption (to be fulfilled by an appropriate design of the control law) that the actual state and input trajectory evolve μ-close to the reference, the previous properties hide a supervisor strategy for choosing the time law so that the system evolves robustly in FF ($\mathfrak{q}(t) \in \Sigma_a'$), or evolves in FF by possibly switching to VI ($\mathfrak{q}(t) \in \Sigma_a$), or definitely switches the operative mode to VI ($\mathfrak{q}(t) \in \Sigma_a''$).

- *b. Sliding reference manoeuvre.* This is the second reference manoeuvre designed to slide along the vertical surface. Mathematically, the reference manoeuvre is a smooth function $\xi_b^\star(\mathfrak{q}(t)) \in \mathcal{D}(VI)$ and a bounded function $u_b^\star(\mathfrak{q}(t)) \in U$ of the form specified in Appendix A, where $\mathfrak{q}(t) \subset \mathbb{R}^3$ is the specific time law. The latter is supposed to range in the set $\Sigma_b \subset \mathbb{R}^3$ that, as above, is chosen along with the geometric path to fulfil a number of properties. Specifically, it is supposed that there exist Σ_b', $\Sigma_b'' \subset \Sigma_b$ such that the following properties, interpretable as we did for (14), hold:

$$\begin{aligned}
&(\mathrm{gr}(\xi_b^\star, u_b^\star)|_{\Sigma_b} + \mathcal{B}_\mu) \bigcap \left(\bigcup_{\{VI,q\}\in\mathcal{E}\setminus\{VI,FF\}} \mathcal{G}(\{VI,q\}) \right) = \emptyset;\\
&(\mathrm{gr}(\xi_b^\star, u_b^\star)|_{\Sigma_b'} + \mathcal{B}_\mu) \bigcap \left(\bigcup_{\{VI,q\}\in\mathcal{E}} \mathcal{G}(\{VI,q\}) \right) = \emptyset;\\
&(\mathrm{gr}(\xi_b^\star, u_b^\star)|_{\Sigma_b''} + \mathcal{B}_\mu) \subset \mathcal{G}(\{VI,FF\}).
\end{aligned} \tag{15}$$

- *c. Undocking reference manoeuvre.* This is the last manoeuvre associated to the final phase in which the vehicle definitely undocks from the vertical surface and evolves in the operative mode FF. Mathematically, the reference manoeuvre is a smooth function $\xi_c^\star(\mathfrak{q}(t)) \in \mathcal{D}(FF)$ and a bounded function $u_c^\star(\mathfrak{q}(t)) \in U$ of the form specified in Appendix A, where $\mathfrak{q}(t) \subset \mathbb{R}^5$ is the specific time law taking value in a set $\Sigma_c \subset \mathbb{R}^5$. The main property required to this manoeuvre is to take place μ-distant from any guard set in order to avoid unplanned switches to others operative modes (such as a further contact with the vertical surface). Geometrically, this condition can be simply expressed as

$$(\mathrm{gr}(\xi^{\star_c}, u_c^\star)|_{\Sigma_c} + \mathcal{B}_\mu) \bigcap \left(\bigcup_{\{FF,q\}\in\mathcal{E}} \mathcal{G}(\{FF,q\}) \right) = \emptyset. \tag{16}$$

The overall docking–undocking manoeuvre is thus the combination of $(\xi_a^\star, u_a^\star)$, $(\xi_b^\star, u_b^\star)$ and $(\xi_c^\star, u_c^\star)$ fulfilling conditions (14)–(16).

3.2. Control synthesis

We present possible low-level control laws for the operative modes FF and VI of interest for the docking–undocking manoeuvre under consideration. The control laws depend on specific reference manoeuvres and are parametrised by the respective time laws. The provided stability properties hold for all possible time laws in a given compact set. This feature allows one, in the selection of the supervisor strategy, to freely choose the most appropriate time law profiles to accomplish desired task without requiring re-design of the controllers.

3.2.1. Free-flight control law

The control law is given in terms of a reference manoeuvre that, according to the path following strategy illustrated above, is written as $(\xi^\star(\mathfrak{q}), u^\star(\mathfrak{q}))$ with $\xi^\star(\mathfrak{q})$ and $u^\star(\mathfrak{q})$ as in (A.1). The time law vector $\mathfrak{q}(t)$ is supposed to be sufficiently smooth and such that $\mathfrak{q}(t) \in \Sigma$ for all t, where Σ is a known set. The set Σ is assumed to be fixed such that for all $\mathfrak{q} \in \Sigma$ the thrust $u_M^\star(\mathfrak{q})$ and the attitude $\theta^\star(\mathfrak{q})$ fulfil the physical constraints $u_M^\star(\mathfrak{q}) \in (\underline{u}_M, \bar{u}_M)$ and $|\theta^\star(\mathfrak{q})| \le \pi/2 - c$, for some $c < \pi/2$.

The proposed inputs u_M (thrust) and u_F (flap's angle of attack) are given by

$$\begin{aligned}
u_M(\mathfrak{q}) &= \frac{1}{\cos\theta}\left(u_M^\star(\mathfrak{q})\cos\theta^\star(\mathfrak{q}) - k_1\tilde{z} + k_2\dot{\tilde{z}}\right)\\
u_F(\mathfrak{q}) &= \frac{1}{u_M(\mathfrak{q})}\Bigg[u_M^\star(\mathfrak{q})u_F^\star(\mathfrak{q}) + K_P\Bigg(K_D\dot{\tilde{\theta}}\\
&\qquad + \tan(\tilde{\theta} + \theta^\star(\mathfrak{q})) - \tan\theta^\star(\mathfrak{q}) + \theta_{\mathrm{out}}\Bigg)\Bigg]
\end{aligned} \tag{17}$$

where $\tilde{z} := z - z^\star(\mathfrak{q})$, $\dot{\tilde{z}} := \dot{z} - \dot{z}^\star(\mathfrak{q})$, $\tilde{\theta} := \theta - \theta^\star(\mathfrak{q})$, $\dot{\tilde{\theta}} := \dot{\theta} - \dot{\theta}^\star(\mathfrak{q})$,

$$\begin{aligned}
&\theta_{\mathrm{out}} := \lambda_2\sigma\left(\frac{K_2}{\lambda_2}\eta\right), \quad \eta := \dot{\tilde{x}} + \lambda_1\sigma\left(\frac{K_1}{\lambda_1}\tilde{x}\right),\\
&\tilde{x} := x - x^\star(\mathfrak{q}), \qquad \dot{\tilde{x}} := \dot{x} - \dot{x}^\star(\mathfrak{q})
\end{aligned} \tag{18}$$

with k_1, k_2, K_P, K_D, and (λ_i, K_i), $i = 1, 2$, design parameters and $\sigma(\cdot)$ a *saturation function* defined as any differentiable function $\sigma : \mathbb{R} \to \mathbb{R}$ satisfying $|\sigma'(s)| := |d\sigma(s)/ds| \le 2$ for all s, $s\sigma(s) > 0$ for all $s \neq 0$, $\sigma(0) = 0$, $\sigma(s) = \mathrm{sgn}(s)$ for $|s| \ge 1$, and $|s| < |\sigma(s)| < 1$ for $|s| < 1$. The proposed control structure rests upon the design idea proposed in Isidori, Marconi, and Serrani (2003), Marconi and Naldi (2007) and, as discussed in those papers, can be interpreted as a *cascade control structure* constituted by an inner loop, controlling the angular $(\theta, \dot{\theta})$ dynamics, and an outer loop governing the lateral $(x, \dot{x})$ and vertical $(z, \dot{z})$ dynamics.

The main properties achievable by the previous controller are detailed in the next proposition that refers to the nominal dynamics (2) perturbed by an additive disturbance $\delta_{FF}(\mathfrak{q})$, i.e.

$$\dot{\xi} = f(FF, \xi, u) + \delta_{FF}(\mathfrak{q}). \tag{19}$$

The disturbance $\delta_{FF}(\mathfrak{q})$ is assumed of the form $\delta_{FF}(\mathfrak{q}) = (0, \delta_{FF,x}, 0, \delta_{FF,z}, 0, 0)^T$ and it is meant to model the effect of neglected

dynamics (such as drag forces, see Section 2.2) and of exogenous disturbances (such as wind-gusts) that might perturb the vehicle in free-flight. It is proved that, for any $\mu > 0$, the proposed controller succeeds in keeping the actual state and input trajectory $(\xi(t), u(t))\mu$-close to any reference manoeuvre characterised by $\mathfrak{q}(t) \in \Sigma$ provided that the initial state of the system is sufficiently close to the initial value of the state manoeuvre, and that δ_{FF} is sufficiently small.

Proposition 1. *Let Σ be a given compact set and assume that $|\theta(0)| \leq \rho < \pi/2$. Let (k_1, k_2) be positive numbers and let (λ_i, K_i) be chosen as $\lambda_i = \epsilon^{i-1}\lambda_i^\star$, $K_i = \epsilon K_i^\star$, $i = 1, 2$, where ϵ is a design parameter and the $\lambda_i^\star$'s and $K_i^\star$'s satisfy*

$$\frac{\lambda_2^\star}{K_2^\star} < \frac{\lambda_1^\star}{4}, \qquad 8K_1^\star\lambda_1^\star < \mu_L\lambda_2^\star, \qquad 24\frac{K_1^\star}{K_2^\star} < \frac{1}{6}\frac{\mu_L}{\mu_U} \tag{20}$$

where $\mu_L = \underline{u}_M \cos(c)$ and $\mu_U = \bar{u}_M$. There exist positive numbers $K_D^\star, K_P^\star(K_D)$ and $\epsilon^\star(K_P)$ such that for any positive $K_D \leq K_D^\star$ and $K_P \geq K_P^\star(K_D)$ and $\epsilon \leq \epsilon^\star(K_P)$ and for all $\mu > 0$, there exist $\Delta_{FF,0}$ and $\Delta_{FF,d}$ such that if

$$|\xi(0) - \xi^\star(\mathfrak{q}(0))| \leq \Delta_{FF,0} \quad \text{and} \quad |\delta_{FF}(\mathfrak{q}(t))| \leq \Delta_{FF,d}$$

for all $\mathfrak{q}(t) \in \Sigma$, then, for the closed-loop system (17) and (19), (18), $|\theta(t)| \leq \pi/2$ and

$$\left|\begin{pmatrix}\xi(t)\\ u(t)\end{pmatrix} - \begin{pmatrix}\xi^\star(\mathfrak{q}(t))\\ u^\star(\mathfrak{q}(t))\end{pmatrix}\right| \leq \mu$$

for all $t \geq 0$, and for all smooth $\mathfrak{q}(t) \in \Sigma$.

The proof of this proposition is in Appendix B. The proof shows how the value of the restrictions $\Delta_{FF,0}$ and $\Delta_{FF,d}$ are mainly affected by the value of μ and ϵ: the larger are μ and ϵ, the larger are $\Delta_{FF,0}$ and $\Delta_{FF,d}$. In this respect we observe that a small value of ϵ is only required to offset critical attitude initial conditions $|\theta(0)|$ close to $\pi/2$ and to avoid that the vehicle overturns (see the first part of the proof). Regarding the practical tuning of the design parameters in (17) and (18), we defer the reader to Section 4.

3.2.2. Vertical interaction control

As motivated in Section 2.2.1, we consider $(\mathcal{F}_1, \mathcal{F}_2)$ as equivalent virtual control inputs related to the physical inputs (u_M, u_F) by relation (10) (well-defined if θ satisfies (5)). The control laws for $(\mathcal{F}_1, \mathcal{F}_2)$ are given in terms of a reference manoeuvre written as $(\xi^\star(\mathfrak{q}), u^\star(\mathfrak{q}))$ with $\xi^\star(\mathfrak{q})$ and $u^\star(\mathfrak{q})$ as in (A.3). The time law vector $\mathfrak{q}(t) \in \mathbb{R}^3$ is supposed to be sufficiently smooth and such that $\mathfrak{q}(t) \in \Sigma$ for all t, where $\Sigma \subset \mathbb{R}^3$ is a known set. Consistently with Appendix A, in view of (5), it is supposed that $\theta^\star(\mathfrak{q})$ satisfies

$$-\gamma_V^M + c_1 \leq \theta^\star(\mathfrak{q}) \leq \gamma_V^F - c_1 \quad \forall\, \mathfrak{q} \in \Sigma \tag{21}$$

for some positive $c_1 < \min\{\gamma_V^F, \gamma_V^M\}$.

The proposed control law is of the form (see (10))

$$\begin{aligned} u_M(\mathfrak{q}) &= \begin{pmatrix}1 & 0\end{pmatrix} G^{-1}(\theta) L(\theta) \begin{pmatrix}\mathcal{F}_1(\mathfrak{q})\\ \mathcal{F}_2(\mathfrak{q})\end{pmatrix},\\ u_F(\mathfrak{q}) &= \frac{1}{u_M(\mathfrak{q})}\begin{pmatrix}0 & 1\end{pmatrix} G^{-1}(\theta) L(\theta) \begin{pmatrix}\mathcal{F}_1(\mathfrak{q})\\ \mathcal{F}_2(\mathfrak{q})\end{pmatrix} \end{aligned} \tag{22}$$

with

$$\begin{aligned} &\mathcal{F}_1(\mathfrak{q}) = \mathcal{F}_1^\star(\mathfrak{q}) - K_P(\tilde{\theta} + K_D\dot{\tilde{\theta}}), \quad \tilde{\theta} := \theta - \theta^\star(\mathfrak{q}),\\ &\mathcal{F}_2(\mathfrak{q}) = \mathcal{F}_2^\star(\mathfrak{q}) - K_P(\tilde{\beta} + K_D\dot{\tilde{\beta}}), \quad \dot{\tilde{\theta}} := \dot{\theta} - \dot{\theta}^\star(\mathfrak{q}),\\ &\tilde{\beta} := \beta - \beta^\star(\mathfrak{q}), \qquad \dot{\tilde{\beta}} := \dot{\beta} - \dot{\beta}^\star(\mathfrak{q}) \end{aligned} \tag{23}$$

where $(\mathcal{F}_1^\star(\mathfrak{q}), \mathcal{F}_2^\star(\mathfrak{q}))$ are as in (A.4) and K_P and K_D are positive design parameters. The stability result presented in the next proposition emphasises the robustness of (23) with respect to uncertainties on the value of the friction parameter λ_V in (9) whose nominal value λ_{V0} has been used to compute the reference manoeuvre (see Appendix A). The statement of the proposition refers to a signal $\delta_{VI}(\mathfrak{q})$ defined as follow

$$\delta_{VI}(\mathfrak{q}) := \frac{\lambda_V - \lambda_{V0}}{M}\,\dot{\beta}^\star(\mathfrak{q}) \begin{pmatrix}\dfrac{\cos(\theta^\star(\mathfrak{q}) + \gamma_V^M)}{\ell_V \sin^2(\theta^\star(\mathfrak{q}) + \gamma_V^M)}\\ \dfrac{1}{\sin^2(\theta^\star(\mathfrak{q}) + \gamma_V^M)}\end{pmatrix}$$

and claims, besides others, that $\theta(t) \in (-\gamma_V^M, \gamma_V^F)$ so that $G^{-1}(\theta)$ and, in turn, (22) are well-defined.

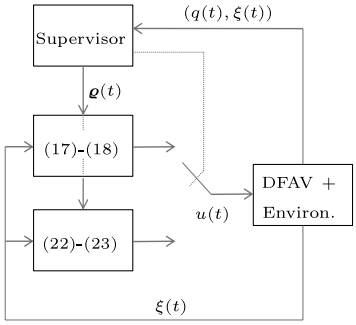

Fig. 3. Control architecture.

Proposition 2. *Let Σ be a fixed compact set and let K_D be an arbitrary positive number. There exists $K_P^\star > 0$ such that for all $K_P \geq K_P^\star$ and $\mu > 0$ there exist positive $\Delta_{VI,0}$ and $\Delta_{VI,d}$ such that if*

$$|\xi(0) - \xi^\star(\mathfrak{q}(0))| \leq \Delta_{VI,0} \quad \text{and} \quad |\delta_{VI}(\mathfrak{q}(t))| \leq \Delta_{VI,d}$$

for all $\mathfrak{q}(t) \in \Sigma$, then, for the closed-loop system (9) and (23), $\theta(t) \in (-\gamma_V^M, \gamma_V^F)$ and

$$\left|\begin{pmatrix}\xi(t)\\ u(t)\end{pmatrix} - \begin{pmatrix}\xi^\star(\mathfrak{q}(t))\\ u^\star(\mathfrak{q}(t))\end{pmatrix}\right| \leq \mu$$

for all $t \geq 0$, and for all smooth $\mathfrak{q}(t) \in \Sigma$.

The proof of this proposition is sketched in Appendix C.

3.3. Design of the supervisor

In the overall control architecture, sketched in Fig. 3, the role of the supervisor is to activate the specific control law (17)–(18) or (22)–(23) according to the actual operative mode of the vehicle, and to feed the controllers with the appropriate time law profile $\mathfrak{q}(t)$ according to the desired task and to the state of the vehicle.

The starting point in the supervisor strategy is the notion of reference manoeuvre that, for the specific docking–undocking task, are given by the three manoeuvres $(\xi_a^\star(\mathfrak{q}), u_a^\star(\mathfrak{q}))$, $(\xi_b^\star(\mathfrak{q}), u_b^\star(\mathfrak{q}))$ and $(\xi_c^\star(\mathfrak{q}), u_c^\star(\mathfrak{q}))$ introduced in Section 3.1, and the resulting FF and VI control laws given in Section 3.2.

By defining $u_{FF}(\mathfrak{q}) := (u_M(\mathfrak{q}), u_F(\mathfrak{q}))$ with $u_M(\mathfrak{q})$ and $u_F(\mathfrak{q})$ given by (17)–(18), and $u_{VI}(\mathfrak{q}) := (u_M(\mathfrak{q}), u_F(\mathfrak{q}))$ with $u_M(\mathfrak{q})$ and $u_F(\mathfrak{q})$ given by (22)–(23), the switching strategy among controllers is simply of the form

$$u(t) = u_{q(t)}(\mathfrak{q}(t)) \tag{24}$$

with $q(t)$, the actual flight mode, taking values in the set $\{FF, VI\}$ and with $\mathfrak{q}(t)$ a degree-of-freedom to be chosen by the supervisor according to the desired task. The value of $q(t)$ is thus assumed to be known. It might come from contact sensors, such as tactile or force sensors, appropriately positioned in the DFMAV structure.

The main result regarding the supervisor is specified in the next proposition. In order to make the statement of the proposition

shorter we fix the underlying framework beforehand. Specifically, let $\Sigma_a \subset \mathbb{R}^5$, $\Sigma_b \subset \mathbb{R}^3$ and $\Sigma_c \subset \mathbb{R}^5$ be fixed compact sets such that properties (14)–(16) are fulfilled for some $\mu > 0$ and some Σ_a', Σ_a'', Σ_b' and Σ_b''. With μ and Σ_a, Σ_b and Σ_c given, let the design parameters of controller (17)–(18) (respectively (22)–(23)) be fixed once and for all according to Proposition 1 (respectively Proposition 2) by considering $\Sigma = \Sigma_a \cup \Sigma_c$ (respectively $\Sigma = \Sigma_b$) so that the properties indicated in the propositions are fulfilled for some positive $(\Delta_{0,FF}, \Delta_{d,FF})$ and $(\Delta_{0,VI}, \Delta_{d,VI})$. Finally, with t_1, t_2, t_3 positive numbers, let $\mathfrak{q}_a(t) : [0, t_1] \to \Sigma_a \subset \mathbb{R}^5$, $\mathfrak{q}_b(t) : [0, t_2] \to \Sigma_b \subset \mathbb{R}^3$, and $\mathfrak{q}_c(t) : [0, t_3) \to \Sigma_c \subset \mathbb{R}^5$ be arbitrary smooth functions with $\mathfrak{q}_a(t)$ and $\mathfrak{q}_b(t)$ satisfying the following properties:

(a) $\mathfrak{q}_a(t) \in \Sigma_a'$ for all $t \in [0, t_1']$, with $t_1' < t_1$, and $\mathfrak{q}_a(t_1) \in \Sigma_a''$;
(b) $\mathfrak{q}_b(t) \in \Sigma_b'$ for all $t \in [0, t_2']$, with $t_2' < t_2$, and $\mathfrak{q}_b(t_2) \in \Sigma_b''$.

In this framework the following result, proved in Appendix D, holds.

Proposition 3. *For all $\xi(0)$ and for all bounded $\delta_{FF}(t)$ fulfilling*

$$|\xi(0) - \xi_a^\star(\mathfrak{q}_a(0))| \le \Delta_{FF,0}, \qquad \|\delta_{FF}\|_\infty \le \Delta_{FF,d}, \tag{25}$$

the closed-loop trajectory obtained by (24) with $\mathfrak{q}(t) = \mathfrak{q}_a(t)$ is such that $|(\xi(t), u(t)) - (\xi_a^\star(\mathfrak{q}_a(t)), u_a^\star(\mathfrak{q}_a(t)))| \le \mu$ (and, as consequence, $q(t) = FF$) for all $t \in [0, t_1']$ and there exists a $t_{s1} \in (t_1', t_1]$ such that $(\xi(t_{s1}), u(t_{s1})) \in \mathcal{G}(\{FF, VI\})$. Furthermore, if

$$|\mathcal{R}(\{FF, VI\}, (\xi(t_{s1}), u(t_{s1}))) - \xi_b^\star(\mathfrak{q}_b(0))| \le \Delta_{VI,0}, \tag{26}$$

then for all bounded $\delta_{VI}(t)$ satisfying $\|\delta_{VI}\|_\infty \le \Delta_{VI,d}$, the closed-loop trajectory obtained by (24) with $\mathfrak{q}(t) = \mathfrak{q}_b(t - t_{s1})$ for $t \ge t_{s1}$ is such that $|(\xi(t), u(t)) - (\xi_b^\star(\mathfrak{q}_b(t - t_{s1})), u_b^\star(\mathfrak{q}_b(t - t_{s1})))| \le \mu$ (and, as a consequence, $q(t) = VI$) for all $t \in [t_{s1}, t_{s1} + t_2']$ and there exists a $t_{s2} \in (t_{s1} + t_2', t_{s1} + t_2]$ such that $(\xi(t_{s2}), u(t_{s2})) \in \mathcal{G}(\{VI, FF\})$. Finally, if

$$|\mathcal{R}(\{VI, FF\}, (\xi(t_{s2}), u(t_{s2}))) - \xi_c^\star(\mathfrak{q}_c(0))| \le \Delta_{FF,0}, \tag{27}$$

then for all bounded $\delta_{FF}(t)$ satisfying $\|\delta_{FF}\|_\infty \le \Delta_{FF,d}$, the closed-loop trajectory obtained by (24) with $\mathfrak{q}(t) = \mathfrak{q}_c(t - t_{s2})$ for $t \ge t_{s2}$ is such that $|(\xi(t), u(t)) - (\xi_c^\star(\mathfrak{q}_c(t - t_{s2})), u_c^\star(\mathfrak{q}_c(t - t_{s2})))| \le \mu$ (and, as a consequence, $q(t) = FF$) for all $t \in [t_{s2}, t_{s2} + t_3)$.

Thus, the overall supervisor control strategy amounts to switch the low-level controller according to the actual state $q(t)$ of the contact sensor ($q = VI$ if a contact is detected, $q = FF$ otherwise) and to choose $\mathfrak{q}(t)$ in a way that its value ranges in the sets Σ_a', Σ_a'', Σ_b', Σ_b'' and Σ_c according to the desired task. Note that, according to Section 3.2, re-design of the controllers is not needed as long as $\mathfrak{q}(t)$ ranges within Σ_a, Σ_b and Σ_c. This fact allows the supervisor to act on $\mathfrak{q}(t)$ to implement "emergency" actions, such as a recovery manoeuvre after a failed docking, without re-designing the geometric path of the reference and re-tuning the low-level controllers. The simulation results in Section 4 give further insight about this point.

Remark. It is worth emphasising that the previous result is local due to the restrictions $\Delta_{FF,0}$ on the initial state characterising (25). Furthermore, the fulfilment of condition (26) (respectively of (27)) requires the ability to generate reference manoeuvres adaptively according to the actual state. Specifically, as the value of the reset state is not known precisely in advance, a bunch of possible $\xi_b^\star(\mathfrak{q}_b(t))$ (respectively $\xi_c^\star(\mathfrak{q}_c(t))$) should be designed beforehand so that at least one reference trajectory, for which (26) ((27)) hold, exists. Practically, the bunch of reference trajectories might be obtained by properly parametrising a nominal reference trajectory, with the value of the parameter that is then selected "on-the-fly" according to the actual reset state.

In the previous framework, a critical point in the enforcement of a successful docking manoeuvre is the selection of $\mathfrak{q}_a(t) \in \Sigma_a''$ satisfying the last in (14). This, in turn, guarantees that the vehicle definitely docks with the vertical surface with an impact that, by definition of Σ_a'' in (14), is inelastic, namely rebounds do not occur. In this respect, by the definition of $\mathcal{G}(FF, VI)$, the critical design step is to identify a time law $\mathfrak{q}_a(t)$ such that the resulting coefficient of restitution $c_R(F_X(\xi_a^\star(\mathfrak{q}_a(t)), u_a^\star(\mathfrak{q}_a(t))), \dot\alpha_V(\xi_a^\star(\mathfrak{q}_a(t))))$ is zero. In the next proposition, proved in Appendix D, we present a result that shows how this condition can be enforced if the impact dynamics are governed by the damped compliant impact model described in Section 2.3.

Proposition 4 (*Rebounds-Free Docking Manoeuvres*)**.** *There exists a $\epsilon^\star > 0$ such that for all positive $\epsilon \le \epsilon^\star$ the following holds*

$$\begin{aligned} 0 \le\ & \dot\alpha_V(\xi_a^\star(\mathfrak{q}_a))^2 \le \epsilon\ F_X(\xi_a^\star(\mathfrak{q}_a), u_a^\star(\mathfrak{q}_a)) \\ & \Rightarrow c_R(F_X(\xi_a^\star(\mathfrak{q}_a), u_a^\star(\mathfrak{q}_a)), \dot\alpha_V(\xi_a^\star(\mathfrak{q}_a))) = 0. \end{aligned} \tag{28}$$

The value of $\epsilon^\star$ predicted by the previous proposition is clearly dependent on dissipative and elastic properties of the impacting material. The impact is thus inelastic if the ratio between the square of the lateral speed of the point P_V and the lateral force F_X at the impact is sufficiently small. As also suggested by intuition, successful docking manoeuvres thus require that the vehicle gets close to the vertical surface at low speed (so that the impact lateral speed is eventually small) and suddenly accelerates just before docking so that the lateral impact force is eventually large. As shown in the simulation section, a practical way to enforce such a manoeuvre is to design time law $\mathfrak{q}_a(t)$ with small $\dot\rho(t)$ and large $\ddot\rho(t)$. It must be noted that, according to the definition of Σ_a'', the value of μ must be small in relation to $\epsilon^\star$ in order to have the last condition in (14) fulfilled with a $\xi_a^\star(\mathfrak{q}_a)$, $u_a^\star(\mathfrak{q}_a)$ satisfying (27). This, in turn, imposes upper bounds in the allowed restrictions $\Delta_{FF,0}$ and $\Delta_{FF,d}$ according to Proposition 1.

Finally, it is worth investigating the effectiveness of the proposed approach when, due to disturbances or impact dynamics behaving differently from the considered model, docking manoeuvres fail and rebounds take place unexpectedly. In these un-ideal scenarios the possible supervisor strategy strongly depends on the resulting reset state $\mathcal{R}(\{FF, FF\}, (\xi(t_{s1}), u(t_{s1})))$. If the reset state is "sufficiently close" to an undocking reference manoeuvre, a possible strategy is to implement a "recovery manoeuvre" steering the vehicle far-off the surface and then to eventually start a further docking manoeuvre. In the proposed setting this strategy is implementable if

$$\min_{\mathfrak{q}_c \in \Sigma_c} \left|\mathcal{R}(\{FF, FF\}, (\xi(t_{s1}), u(t_{s1}))) - \xi_c^\star(\mathfrak{q}_c)\right| \le \Delta_{FF,0}. \tag{29}$$

In such a case, denoting by $\bar{\mathfrak{q}}_c$ any element of Σ_c at which the previous minimum is attained, and with $\mathfrak{q}_c(t)$ any smooth time law in Σ_c with $\mathfrak{q}_c(t_{s1}) = \bar{\mathfrak{q}}_c$, the possible supervisor strategy is to take (24) with $\mathfrak{q}(t) = \mathfrak{q}_c(t)$. Indeed, in such a case, the same arguments of Proposition 3 lead to conclude that $q(t) \equiv FF$ and the undocking reference manoeuvre is tracked with an error bounded by μ. In all the cases in which the reset state is not sufficiently close to an undocking reference manoeuvre, the proposed recovering action cannot be implemented. In these situations, the proposed strategy cannot prevent undesired behaviours such as reiterated rebounds leading towards a Zeno behaviour of the hybrid system, Goebel et al. (2009). Emergency control actions should be then implemented at supervisor level whose design, though, is not addressed in this paper.

4. Simulation results

We consider the DFMAV dynamical model described in Naldi et al. (2010) with $M = 1.5$ kg, $\ell_V = 0.5$ m, $d_V = 0.5$ m, $\gamma_V^M = \gamma_V^F = \pi/4$, $\lambda_x = 1$ Ns/m, $\lambda_{x0} = 0.5$ Ns/m, $k_F = 1$, $J = 0.015$ kgm^2, $\bar u_F = 0.5$ rad, $\bar u_M = 2$ Mg and $\underline{u}_M = 1$ N. In the

VI mode, we considered $\lambda_{V0} = 7$ Ns/m for control purposes and we run the simulations with a more advanced friction model. In particular, following Harnoy et al. (2008), the Coulomb friction has been approximated by $\mu_c F_X(1 - \exp(-\dot\beta^2/a^2))$ with $\mu_c = 0.65$ and $a = 0.1$, where the force F_X represents the normal force to the surface.

4.1. Impact modelling

By bearing in mind the notations in Section 2.3, we fixed $\bar c_R = 0.5$, $k_e = 1600$ N/m and $k_d = 50$ Ns/m and we approximated the impact duration δT_i with the settling time (5%) of (12) given by 0.1 s. With the above values, $c_R(F_X, \alpha_V)$ can be computed for any pair $F_X(t_i)$ and $\dot\alpha_V(t_i)$ by solving the linear ODE (12). The value of c_E entering in $\mathcal{R}(\{FF, FF\}, (\xi, u))$ and $\mathcal{R}(\{FF, VI\}, (\xi, u))$ (see Section 2.3) has been chosen equal to 0.5.

4.2. Docking, sliding and undocking reference manoeuvres

We consider a fixed vertical reference, i.e. $z^{\star(i)} \equiv 0$, $i \geq 1$, and $x^\star(t) = \varrho(t)$, with the time law $\mathfrak{q}(t) = (\varrho(t), \dot\varrho(t), \ldots, \varrho^{(4)}(t))$ characterised by $\varrho^{(3)}(t) = \varrho^{(4)}(t) \equiv 0$ and by setting piecewise constant acceleration profiles $\ddot\varrho(t)$ in order to govern speed and, in turn, position of the lateral reference signal. Reference signals for position, speed and acceleration have been settled to fulfil the constraints $|\varrho| \leq 20$ m, $|\dot\varrho| \leq 5$ m/s and $|\ddot\varrho| \leq 5$ m/s^2, which, along with additional relations introduced below, contribute to define the sets Σ_a and Σ_c. Regarding the docking manoeuvre, the lateral position $\bar\alpha$ of the vertical surface (see Fig. 1) is assumed to fulfil $\bar\alpha_L < \bar\alpha < \bar\alpha_U$, with $\bar\alpha_L = 4.9$ m and $\bar\alpha_U = 5.1$ m. Thus, the set Σ_a' in Section 3.1 can be completely determined by the additional relation $\varrho + \ell_V \cos(\theta^\star(\mathfrak{q}) + \gamma_V^M) \leq \bar\alpha_L - c_x(\mu)$, with $\theta^\star(\mathfrak{q})$ defined in (A.2) and $c_x(\mu)$ a positive constant (with μ introduced in Section 3.1) taken equal to 0.1. Indeed, whenever $\mathfrak{q} \in \Sigma_a'$, the lateral reference position of P_{V1} is guaranteed to be on the left of the surface and the UAV to be robustly in the FF mode provided that the lateral position of P_{V1} follows the reference with an error bounded by $c_x(\mu)$. On the other hand, the definition of the set Σ_a'' requires that the time law is chosen so that $\varrho + \ell_V \cos(\theta^\star(\mathfrak{q}) + \gamma_V^M) \geq \bar\alpha_U + c_x(\mu)$ and that the additional relations $F_X > 0$ (lateral force pointing inward the vertical surface) and $c_R = 0$ (inelastic impact) are fulfilled. The relations in Appendix A and the fact that $\varrho^{(3)} = \varrho^{(4)} = 0$, show that

$$F_X(\theta^\star(\mathfrak{q}), u_M^\star(\mathfrak{q}), u_F^\star(\mathfrak{q})) = M(1 + c\,\varsigma(\dot\varrho, \ddot\varrho))\,\ddot\varrho + \lambda_x(1 + c\,\varsigma(\dot\varrho, \ddot\varrho))\,\dot\varrho \tag{30}$$

where $c = 2JMgk_f\lambda_x^2/k_\tau$ and

$$\varsigma(\dot\varrho, \ddot\varrho) = \ddot\varrho^2 \cos\theta^\star(\mathfrak{q})/[(Mg)^2 + (M\ddot\varrho + \lambda_x\dot\varrho)^2]^2 > 0.$$

Hence, a positive F_X is enforced with positive $\dot\varrho$ or $\ddot\varrho$. On the other hand, by the discussion in Section 4.1, the enforcement of $c_R = 0$ asks that the lateral reference speed of P_{V1}, equal to $\dot\varrho - \ell_V \sin(\theta^\star(\mathfrak{q}) + \gamma_V^M)\dot\theta^\star(\mathfrak{q})$, is small in relation to the value of (30) at the impact time. This, in turn, asks that the time law, at the impact time, is characterised by a small $\dot\varrho$ and large $\ddot\varrho$, with numerical values that can be estimated by using the values chosen above for k_e, k_d and λ_x. The definition of the set Σ_a'' can be thus completed by requiring that $0 \leq \dot\varrho \leq c_v(\mu)$ and $\ddot\varrho \geq c_F(\mu)$, with $c_v(\mu)$ and $c_F(\mu)$ chosen as $c_v(\mu) = 0.3$ m/s and $c_F(\mu) = 0.2$ m/s^2. Regarding the undocking manoeuvre, the definition of $\mathcal{G}(\{VI, FF\})$ and the relations above suggest to take time laws resulting in negative lateral reference forces (i.e. forces pointing outward the vertical surface), namely negative $\ddot\varrho$ and $\dot\varrho$. Accordingly, the set Σ_c in Section 3.1 has been fixed by requiring $\dot\varrho < 0$ and $\ddot\varrho < -c_F(\mu)$.

We describe now the sliding reference manoeuvre. In the first part of the manoeuvre reference trajectories characterised by a constant angle $\theta^\star$, i.e. $\theta^{\star(i)} = 0$ for $i = 1, 2$, and a vertical reference of the form $\beta^\star(\varrho(t)) = \varrho(t)$, with $\mathfrak{q}(t) = (\varrho(t), \dot\varrho(t), \ddot\varrho(t))$ assumed to fulfil $|\varrho| \leq 10$ m, $|\dot\varrho| \leq 2$ m/s and $|\ddot\varrho| \leq 1$ m/s^2 in the definition of Σ_b, have been considered. The definition of the set Σ_b' (see Section 3.1) has been then completed by limiting $\mathfrak{q}$ to those values that guarantee a sufficiently positive $F_X(\theta^\star, u_M^\star, u_F^\star)$. By using the relation in Appendix A, a numerical evaluation of $F_X(\theta^\star, u_M^\star, u_F^\star)$ in terms of $\mathfrak{q}$ shows that if $\theta^\star \in [0.05, 0.1]$ rad, a possible definition of Σ_b' is with $\dot\varrho \in [0, 1]$ m/s and $\ddot\varrho \in [-1, 1]$ m/s^2. This guarantees that the UAV remains in contact with the surface provided that the actual trajectory is sufficiently close to the reference. The final part of the manoeuvre has been obtained by considering a constant $\beta^\star$, i.e. $\beta^{\star(i)} = 0$ for $i = 1, 2$, and $\theta^\star(\varrho(t)) = \varrho(t)$ with $\mathfrak{q}(t) = (\varrho(t), \dot\varrho(t), \ddot\varrho(t))$ constrained to a set Σ_b'' fixed so that $F_X(\theta^\star, u_M^\star, u_F^\star) < 0$. In this respect a numerical inspection of $F_X(\theta^\star, u_M^\star, u_F^\star)$ revealed that a possible definition of Σ_b'' is with $\varrho \in [-0.3, -0.1]$ rad, $\dot\varrho \in [-3.0, 0]$ rad/s and $\ddot\varrho \in [-12, -8]$ rad/s^2. This choice of high values for the angular acceleration, still compatible with the input constraints, allows the UAV to enter the guard set $\mathcal{G}(\{VI, FF\})$ with a negative pitch angle θ.

The initial condition of the time law of the above manoeuvres have been taken so that the difference between the reference signal at the time in which a transition takes place and the actual state resulting from a reset map is minimised. This, in turn, makes the concatenation conditions (26) and (27) satisfied.

4.3. Tuning of the controllers

With $(\Sigma_a, \Sigma_b, \Sigma_c)$ fixed, we present now a few practical steps followed to tune the FF and VI controllers of Section 3.2. We start with the FF controller (17). According to the proof of Proposition 1, the first step regards the choice of (k_1, k_2) chosen equal to (10, 10) so that system (B.1) is ISS. Simulative tests have been done on system (B.1) with δ_{FF} taken constant ($= 0.25\,\bar u_M$) in order to estimate a bound of $\tilde v_1 = -k_1\tilde z_1 - k_2\dot{\tilde z}_2$ (to be used in the sequel).

As second step, we focused on the $\tilde\theta$-subsystem of (B.2) to obtain a lower bound $K_D^\star$ and $K_P^\star$ on the gains and an upper bound $\theta_{\text{out}}^\star$ on the amplitude of the (saturated) outer-loop controller. According to the proof of Proposition 1, the lower and upper bounds have been computed so that, given an estimation of the initial attitude state $\theta(0)$ and of $(\tilde\theta_1(0), \dot{\tilde\theta}_2(0))$, the vehicle does not overturn. At this stage the tuning has been done by simulating the $\tilde\theta$-subsystem of (B.2) with θ_{out} constant and by considering initial conditions fulfilling $|\theta(0)| \leq 30$ deg, $|\tilde\theta_1(0)| \leq 30$ deg and $|\tilde\theta_2(0)| \leq 10$ deg/s. Numerically, we found $(K_D^\star, K_P^\star) = (0.2, 3.5)$ and $\theta_{\text{out}}^\star = 1$ as satisfactory values. Then we focused on system (B.3)–(B.4) and on (20). Following Isidori et al. (2003), let $(\lambda_i^\star, K_i^\star)$ be defined as $\lambda_2^\star = \ell^2\lambda_1^\star/8$, $K_i = \ell^i$, $i = 1, 2$, in which $\lambda_1^\star$ is an arbitrary positive number and $\ell > 0$. It turns out that Eq. (20) are fulfilled with ℓ sufficiently large for any μ_L and μ_U. With an estimation of (μ_L, μ_U) in hand, we fixed $\ell = 5$ and $\lambda_1^\star = 1$ and started to simulate system (B4)–(B5) considering constant exogenous inputs $(\tilde v_1, \delta_{FF,x}(\mathfrak{q}))$. The value of $\tilde v_1$ has been fixed at the upper bound found while tuning the vertical controller above, while $\delta_{FF,x}(\mathfrak{q}) = 0.25 \cdot \bar u_M$. With the values of K_P and K_D found above, we thus checked, by simulation, the boundedness of the trajectories of system (B4)–(B5) and we finally fixed $\epsilon = 0.5$ so that $\epsilon < \theta_{\text{out}}^\star/\lambda_2^\star$ (as required by the proof of Proposition 1).

The tuning of the VI controller detailed in Section 3.2.2 is less involved as it amounts to tune the gain K_P and K_D so that (C.1)–(C.2) has bounded trajectories. By considering a mismatch of 30% between actual and nominal value of the friction coefficient (by thus estimating $\delta_{VI}(\mathfrak{q})$), we found, by simulation, the values $(K_P, K_D) = (100, 0.2)$.

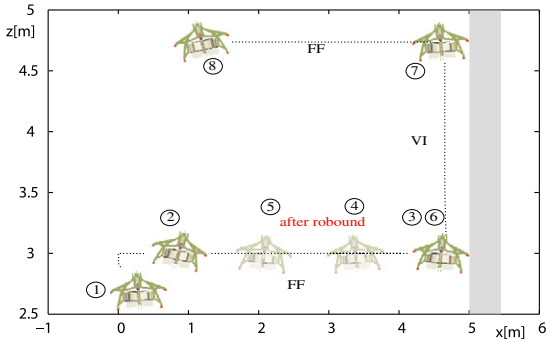

Fig. 4. The graph of the overall manoeuvre in the $X - Z$ space. The rigid vertical surface is located at $x = 5$ m.

4.4. Simulated manoeuvres

The simulation results have been obtained by implementing (24) with $q(t) = FF$ if $x(t) + \ell_V \cos(\theta(t) + \gamma_V^M) < \bar{\alpha}$ and $q(t) = VI$ otherwise. The overall simulated manoeuvre in the longitudinal-vertical plane is shown in Fig. 4, where a graphical sketch of the aircraft altitude is also given. At time $t = 0$ we set $(x(0), \dot{x}(0)) = (0.1, 0)$, $(z(0), \dot{z}(0)) = (2.8, 0)$, $(\theta(0), \dot{\theta}(0)) = (0, 0)$. In the first 10 s the supervisor imposes $\mathfrak{q}_a \in \Sigma_a$ given by $\mathfrak{q}_a(t) \equiv 0$ and $z^\star \equiv 3$ so that a hovering manoeuvre at $(x, z) = (0, 3)$ is performed. After 10 s of hovering, the time law is changed by imposing a lateral constant acceleration $\ddot{\varrho} = 2$ m/s^2 that is then set to zero at $t = 10.5$ s to reach a final speed of 1 m/s. The resulting reference trajectory leads the vehicle to hit the vertical surface at $t = t_{i1} \approx 14.9$ s with an impact that, due to the values of $F_X(t_{i1})$ (≈ 1 N) and $\dot{\alpha}_V(t_{i1})$ (≈ 1 m/s), is elastic. As a consequence the aerial robot rebounds by reaching again the FF configuration with a state given by $\mathcal{R}(\{FF, FF\}, (\xi(t_{i1}), u(t_{i1})))$. The supervisor detects this anomalous situation (deliberately imposed in order to test unwanted rebounds) and instantaneously imposes a constant $\ddot{\varrho} = -5$ m/s (i.e. an undocking reference manoeuvre compatible with condition (29)) by setting $(\varrho(t_{i1}^+), \dot{\varrho}(t_{i1}^+)) = (x(t_{i1}^+), \dot{x}(t_{i1}^+))$ in order to move the UAV away from the surface reaching a lateral speed of -0.5 m/s. At $t = 17$ s a different docking manoeuvre is initiated. Firstly, the time law $\mathfrak{q}_a$ is chosen in the set Σ_a' to approach the vertical surface with small constant speed $\dot{\varrho} = 0.1$ m/s and zero acceleration. When the UAV is 0.45 m far from the nominal position of the surface (so that even considering the 0.1 m uncertainties the point P_{V1} is still not in contact), the value of $\ddot{\varrho}$ is set to 0.2 m/s^2 in order to enforce an impact with a large ratio $F_X/\dot{\alpha}_V$. Indeed, the impact takes place at $t = t_{i2} \approx 27.9$ s with a speed $\dot{\alpha}_v \approx 0.22$ m/s and a lateral force $F_X \approx 0.57$ N. By computing $c_R(F_x, \dot{\alpha}_V)$, the impact is inelastic. The reference trajectories $x^\star$, $z^\star$ and $\theta^\star$ and the tracking errors of this first part of the simulation are shown in Fig. 5. The control inputs are depicted in Fig. 7.

From $t = t_{i2}$ the supervisor switches on the VI controller and sets a $\mathfrak{q}_b(t_{i2}) \in \Sigma_b'$ so that $(\varrho(t_{i2}^+), \dot{\varrho}(t_{i2}^+)) = (\beta(t_{i2}^+), \dot{\beta}(t_{i2}^+))$ and $\theta^\star = \theta(t_{i2}^+)$. In the time interval $[t_{i2}, t_{i2} + 6]$ s the time law $\mathfrak{q}_b(t)$ is chosen in Σ_b' according to a trapezoidal profile $\ddot{\varrho}$, with the vehicle that is first accelerated in order to reach a vertical speed of about 0.5 m/s and then decelerated to get zero vertical speed at $t = t_1 \approx 33.9$ s. The fact that $\mathfrak{q}_b(t) \in \Sigma_b'$ guarantees that the manoeuvre is accomplished with a positive lateral force by thus preserving the contact with the surface. At $t = t_1 + 2$ the undocking manoeuvre starts with $\beta^\star$ kept constant at $\beta(t_1)$ and $\theta^\star(t) = \varrho(t)$ with $\mathfrak{q}_b(t)$ chosen in Σ_b in such a way to approach the set Σ_b''. Specifically, a constant $\ddot{\varrho} = -10$ rad/s^2 is imposed with $(\dot{\varrho}(t_1), \varrho(t_1)) = (0, \theta(t_1))$. As a result, the UAV starts rotating and the resulting lateral force F_X decreases with the guard set $\mathcal{G}(\{VI, FF\})$ that is definitely entered at $t = t_2 \approx 36.1$ s with

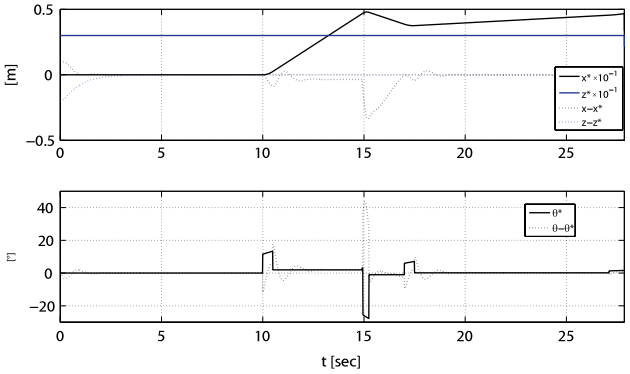

Fig. 5. The references and the tracking errors obtained during the free-flight docking manoeuvres.

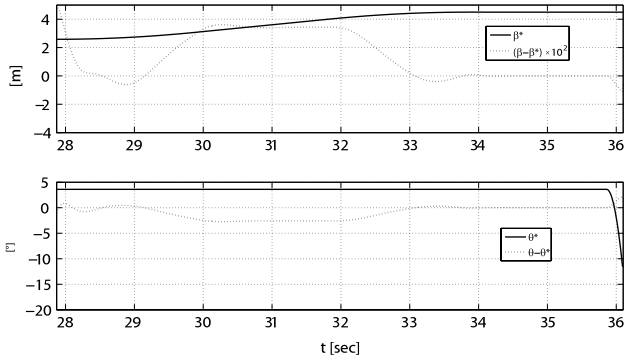

Fig. 6. The references and the tracking errors obtained during the sliding manoeuvre.

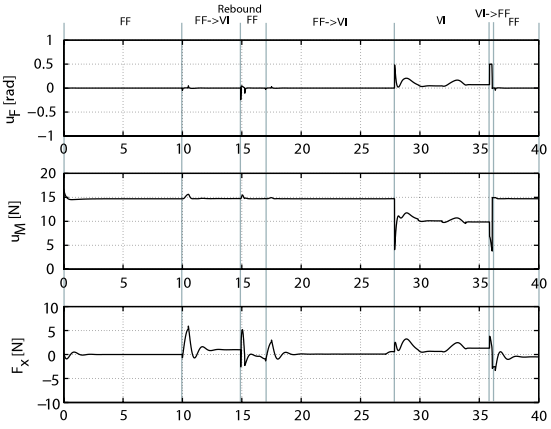

Fig. 7. The control inputs and the force F_X during the manoeuvre.

$\theta(t_2) \approx -11°$. At time t_2 the FF controller is switched on again and an undocking manoeuvre with $\mathfrak{q}_c \in \Sigma_c$ is enforced by the supervisor. The manoeuvre is characterised by a constant $\ddot{\varrho} = -2$ m/s with $(\dot{\varrho}(t_2), \varrho(t_2)) = (\dot{x}(t_2), x(t_2))$ and $z^\star(t) \equiv z(t_2)$ that is then set to zero once the velocity reaches -0.5 m/s. Fig. 6 shows the reference trajectories $\beta^\star$ and $\theta^\star$ in the VI mode and the tracking errors. In Fig. 8 the references $x^\star(t)$, $z^\star(t)$, $\theta^\star(t)$ and the tracking errors in the operative mode *FF* during the undocking manoeuvre are shown.

5. Conclusions

This work has investigated the problem of modelling and controlling an aerial robot interacting with the environment to accomplish missions like inspection of infrastructures, sample

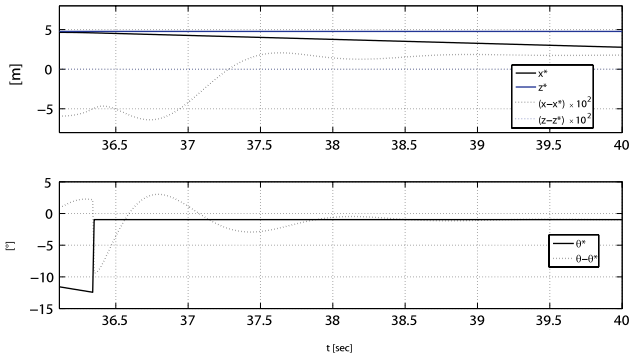

Fig. 8. The references and the tracking errors obtained during the undocking manoeuvre.

picking, etc. The airframe is given by a miniature ducted-fan aerial vehicle able to safely interact with the surrounding environment. Interaction with a vertical surface has been considered and the system has been modelled as a hybrid automaton. A path following strategy has been used to develop a control architecture able to obtain the desired docking–undocking operations by considering a compliant impact model for which the proposed design guarantees the impacts to be completely inelastic. Possible non completely inelastic impacts resulting in "rebounds" of the UAV while docking the surface have been also considered, pointing out the limitations of the proposed approach and the need of future investigations to properly address these unideal circumstances. Simulation results have been shown to validate the proposed framework and the design.

Future work will be focused also on experimental validation of the proposed framework. The accomplishment of this goal will require an important technological effort, in order to match the requirements in term of onboard instrumentations and mechanical design.

Acknowledgments

The authors wish to thank an anonymous reviewer for valuable suggestions provided during the review of the paper.

Appendix A. FF and VI system inversion

FF reference manoeuvre. The reference manoeuvre $(\xi^\star(\mathfrak{q}), u^\star(\mathfrak{q}))$ is given by

$$\begin{aligned}\xi^\star(\mathfrak{q}) &= \mathrm{col}(x^\star(\mathfrak{q}), \dot{x}^\star(\mathfrak{q}), z^\star(\mathfrak{q}), \dot{z}^\star(\mathfrak{q}), \theta^\star(\mathfrak{q}), \dot{\theta}^\star(\mathfrak{q})),\\ u^\star(\mathfrak{q}) &= (u_M^\star(\mathfrak{q}), u_F^\star(\mathfrak{q}))\end{aligned} \tag{A.1}$$

where $x^\star(\mathfrak{q}), \dots, u_F^\star(\mathfrak{q})$ are smooth functions obtained by inverting the dynamics (2). More specifically, let $x^\star(\varrho)$ and $z^\star(\varrho)$ be arbitrary smooth functions. Then $x^\star(\mathfrak{q}) = x^\star(\varrho), z^\star(\mathfrak{q}) = z^\star(\varrho), \dot{x}^\star(\mathfrak{q}) := dx^\star(\varrho)/d\varrho\,\dot{\varrho}, \dot{z}^\star(\mathfrak{q}) := dz^\star(\varrho)/d\varrho\,\dot{\varrho}$, and $\theta^\star(\mathfrak{q})$ can be computed as

$$\theta^\star(\mathfrak{q}) = \arctan\frac{M\ddot{x}^\star(\mathfrak{q}) - \lambda_x\dot{x}^\star(\mathfrak{q})}{M\ddot{z}^\star(\mathfrak{q}) + Mg}. \tag{A.2}$$

With the expression of $\theta^\star(\mathfrak{q})$ (and thus of $\dot{\theta}^\star(\mathfrak{q})$ and $\ddot{\theta}^\star(\mathfrak{q})$) in hand, $u_M^\star(\mathfrak{q})$ and $u_F^\star(\mathfrak{q})$ can be finally computed as

$$u_M^\star(\mathfrak{q}) = \frac{M}{\cos\theta^\star(\mathfrak{q})}\left(\ddot{z}^\star(\mathfrak{q}) + g\right), \qquad u_F^\star(\mathfrak{q}) = -\frac{J\ddot{\theta}^\star(\mathfrak{q})}{k_\tau u_M^\star(\mathfrak{q})}.$$

As $\theta^\star(\mathfrak{q}) = \theta^\star(\varrho, \dot{\varrho}, \ddot{\varrho}), \dot{\theta}^\star(\mathfrak{q}) = \dot{\theta}^\star(\varrho, \dots, \varrho^{(3)})$ and $\ddot{\theta}^\star(\mathfrak{q}) = \ddot{\theta}^\star(\varrho, \dots, \varrho^{(4)})$, note that Eq. (13) is thus solved with $s = 5$.

VI reference manoeuvre. In this case the reference manoeuvre $(\xi^\star(\mathfrak{q}), u^\star(\mathfrak{q}))$ is given by

$$\begin{aligned}\xi^\star(\mathfrak{q}) &= \mathrm{col}(\beta^\star(\mathfrak{q}), \dot{\beta}^\star(\mathfrak{q}), \theta^\star(\mathfrak{q}), \dot{\theta}^\star(\mathfrak{q})),\\ u^\star(\mathfrak{q}) &= (u_M^\star(\mathfrak{q}), u_F^\star(\mathfrak{q}))\end{aligned} \tag{A.3}$$

where $\beta^\star(\mathfrak{q}), \dots, u_F^\star(\mathfrak{q})$ are smooth functions obtained by inverting the dynamics (9) and (10). Specifically, let $\beta^\star(\varrho)$ and $\theta^\star(\varrho)$ be arbitrary smooth functions with $-\gamma_V^M + c_1 \le \theta^\star(\varrho) \le \gamma_V^F - c_1$ for some positive $c_1 < \min\{\gamma_V^F, \gamma_V^M\}$. Then $\beta^\star(\mathfrak{q}) = \beta^\star(\varrho), \theta^\star(\mathfrak{q}) = \theta^\star(\varrho), \dot{\beta}^\star(\mathfrak{q}) := d\beta^\star(\varrho)/d\varrho\,\dot{\varrho}$ and $\dot{\theta}^\star(\mathfrak{q}) := d\theta^\star(\varrho)/d\varrho\,\dot{\varrho}$. Furthermore, by letting

$$\begin{aligned}\mathcal{F}_1^\star(\mathfrak{q}) &:= \ddot{\theta}^\star(\mathfrak{q}) + \ell_\theta(\theta^\star(\mathfrak{q}), \dot{\theta}^\star(\mathfrak{q}), \beta^\star(\mathfrak{q}), \lambda_{V0})\\ \mathcal{F}_2^\star(\mathfrak{q}) &:= \ddot{\beta}^\star(\mathfrak{q}) + \ell_\beta(\theta^\star(\mathfrak{q}), \dot{\theta}^\star(\mathfrak{q}), \beta^\star(\mathfrak{q}), \lambda_{V0}),\end{aligned} \tag{A.4}$$

it turns out that

$$u_M^\star(\mathfrak{q}) = \begin{pmatrix}1 & 0\end{pmatrix} G^{-1}(\theta^\star(\mathfrak{q}))L(\theta^\star(\mathfrak{q}))\begin{pmatrix}\mathcal{F}_1^\star(\mathfrak{q})\\ \mathcal{F}_2^\star(\mathfrak{q})\end{pmatrix}$$

$$u_F^\star(\mathfrak{q}) = \frac{1}{u_M^\star(\mathfrak{q})}\begin{pmatrix}0 & 1\end{pmatrix} G^{-1}(\theta^\star(\mathfrak{q}))L(\theta^\star(\mathfrak{q}))\begin{pmatrix}\mathcal{F}_1^\star(\mathfrak{q})\\ \mathcal{F}_2^\star(\mathfrak{q})\end{pmatrix}.$$

As $\ddot{\theta}^\star(\mathfrak{q}) = \ddot{\theta}^\star(\varrho, \dot{\varrho}, \ddot{\varrho})$ and $\ddot{\beta}^\star(\mathfrak{q}) = \ddot{\beta}^\star(\varrho, \dot{\varrho}, \ddot{\varrho})$, Eq. (13) is thus solved with $s = 3$. It is worth emphasising how, in (A.4), the nominal value λ_{V0} of the friction coefficient has been used.

Appendix B. Proof of Proposition 1

The proof strongly relies upon the arguments and tools proposed in Isidori et al. (2003) and already used in Marconi and Naldi (2007) to control the helicopter dynamics. We consider first the vertical dynamics in (2) controlled by u_M in (17) given by

$$M\ddot{\tilde{z}} = -k_1\tilde{z} - k_2\dot{\tilde{z}} + \delta_{FF,z}(\mathfrak{q}) \tag{B.1}$$

that is clearly input-to-state stable with respect to the input $\delta_{FF,z}$ as k_1 and k_2 are positive numbers.

We turn now our attention on the lateral and angular dynamics in (2) controlled by u_F in (17). The error dynamics read as

$$\begin{aligned}M\ddot{\tilde{x}} &= (\tan(\tilde{\theta} + \theta^\star(\mathfrak{q})) - \tan\theta^\star(\mathfrak{q}))\cos\theta^\star(\mathfrak{q})u_M^\star(\mathfrak{q})\\ &\quad - \lambda_x\dot{\tilde{x}} + \tan\theta(t)\tilde{v}_1 + \delta_{FF,x}(\mathfrak{q})\\ J\ddot{\tilde{\theta}} &= -k_\tau K_P(K_D\dot{\tilde{\theta}} + \tan(\tilde{\theta} + \theta^\star(\mathfrak{q})) - \tan\theta^\star(\mathfrak{q}) + \theta_{\mathrm{out}})\end{aligned} \tag{B.2}$$

in which $\tilde{v}_1 = -k_1\tilde{z} - k_2\dot{\tilde{z}}$. As a first step, it is possible to prove that, by an appropriate tuning of the controller, the DFMAV does not overturn (namely $|\theta(t)| < \pi/2$ for all $t \ge 0$) and $\tilde{\theta}(t)$ can be driven to arbitrarily small values in an arbitrarily small time $T^\star$. The arguments, omitted for reasons of space, follow the ones presented in Isidori et al. (2003, Proposition 5.7.1) and Marconi and Naldi (2007, Proposition 3), and use the crucial fact the $\tilde{\theta}$-subsystem in (B.2) can be regarded, in an initial time interval, as an *autonomous* system driven by the signal $\theta_{\mathrm{out}}(t)$ that is bounded due to the saturation. This and classical high-gain arguments lead to the result that given any $T^\star > 0$ and any $\varepsilon > 0$, there exist $K_D^\star, K_P^\star(K_D)$ and $\theta_{\mathrm{out}}^\star(K_D, K_P)$, such that for any positive $K_D \le K_D^\star, K_P \ge K_P^\star(K_D)$ and $\theta_{\mathrm{out}}(t)$ such that $\|\theta_{\mathrm{out}}\|_\infty \le \theta_{\mathrm{out}}^\star(K_D, K_P)$, and any $\mathfrak{q}(t) \in \Sigma, |\theta(0)| \le \rho \Rightarrow |\theta(t)| < \pi/2$ for all $t \ge 0$ and $|\tilde{\theta}(t)| \le \varepsilon$ for all $t \ge T^\star$.

For $t \ge T^\star$ the interconnection (B.2) is studied. By defining the change of variables $\tilde{\theta} \mapsto \eta_1 := \tan(\tilde{\theta} + \theta^\star(\mathfrak{q})) - \tan\theta^\star(\mathfrak{q}) + \theta_{\mathrm{out}}, \dot{\tilde{\theta}} \mapsto \eta_2 := \dot{\tilde{\theta}} + \eta_1/K_D, \tilde{x} \mapsto \xi_1 := \tilde{x}$ and $\dot{\tilde{x}} \mapsto \xi_2 := \eta$ system (B.2) transforms as the interconnection of system

$$\begin{aligned}\dot{\xi}_1 &= -\lambda_1\sigma\left(K_1\frac{\xi_1}{\lambda_1}\right) + \xi_2\\ M\dot{\xi}_2 &= u_M^\star(\mathfrak{q})\cos\theta^\star(\mathfrak{q})\left(-\lambda_2\sigma\left(K_2\frac{\xi_2}{\lambda_2}\right) + \eta_1\right)\\ &\quad - \lambda_x\xi_2 + \lambda_x\lambda_1\sigma\left(K_1\frac{\xi_1}{\lambda_1}\right) + MK_1\sigma'\left(K_1\frac{\xi_1}{\lambda_1}\right)\dot{\xi}_1\\ &\quad + \tan\theta(t)\tilde{v}_1 + \delta_{FF,x}(\mathfrak{q})\end{aligned} \tag{B.3}$$

with states (ξ_1, ξ_2), inputs $(\eta_1, \tan\theta(t)\tilde{v}_1, \delta_{FF,x}(\mathfrak{q}))$ and outputs $(\theta_{\text{out}}(\xi_2), y_\xi)$ where

$$y_\xi = \dot{\theta}_{\text{out}} - \frac{1}{M}K_2\sigma'\left(K_2\frac{\xi_2}{\lambda_2}\right)\cos\theta^\star(\mathfrak{q})u_M^\star(\mathfrak{q})\eta_1,$$

and a second system of the form

$$\begin{aligned}\dot{\eta}_1 &= \frac{1}{\cos^2\theta(t)}\left(-\frac{\eta_1}{K_D}+\eta_2\right)+L(\eta_1,\theta_{\text{out}},\mathfrak{q})\\ &\quad+\frac{1}{M}K_2\sigma'\left(K_2\frac{\xi_2}{\lambda_2}\right)\cos\theta^\star(\mathfrak{q})u_M^\star(\mathfrak{q})\eta_1+y_\xi \qquad \text{(B.4)}\\ J\dot{\eta}_2 &= -k_\tau K_P K_D\eta_2+\frac{1}{K_D}\dot{\eta}_1\end{aligned}$$

where $L(\eta_1,\theta_{\text{out}},\mathfrak{q}) := \left(1/\cos^2\theta - 1/\cos^2\theta^\star(\mathfrak{q})\right)\dot{\theta}^\star(\mathfrak{q}), \theta = \tan^{-1}(\eta_1+\tan\theta^\star(\mathfrak{q})-\theta_{\text{out}})$, with state (η_1,η_2), inputs $(\theta_{\text{out}}, y_\xi)$ and output η_1. Note that, in the $\dot{\xi}_2$ expression, $u_M^\star(\mathfrak{q})\cos\theta^\star(\mathfrak{q}) \geq \underline{u}_M\cos c > 0$ for all $\mathfrak{q}\in\Sigma$. This interconnection, with (K_i,λ_i), $i=1,2$, chosen as suggested in the proposition, has been studied in Isidori et al. (2003, Lemma 5.7.4), (see also Marconi & Naldi, 2007, Proposition 4) where it has been proved that there exist $R>0$, $K_D^\star$ and $K_P^\star(K_D)$ such that for any positive $K_D \leq K_D^\star$, $K_P \geq K_P^\star(K_D)$ and $\epsilon > 0$ the previous interconnection is ISS with restrictions $(\epsilon R, \epsilon R)$ on the inputs $(\tan\theta(t)\tilde{v}_1, \delta_{FF,x}(\mathfrak{q}))$, no restrictions on the initial state and linear asymptotic gains. From this, by choosing $\epsilon < \theta^\star_{\text{out}}/\lambda_2^\star$, and by cascade arguments, it turns that the overall lateral-longitudinal-vertical system is ISS with restriction on the initial state and restriction on the input δ_{FF} (see Propositions 5 and 6 in Marconi & Naldi, 2007). From now on all the design parameters are fixed as indicated above. In order to complete the proof, the crucial point is to show that the overall lateral-longitudinal-vertical system admits an ISS Lyapunov function *independent of* $\mathfrak{q}$. To this end, we start by noting that $u_M^\star(\mathfrak{q})\cos\theta^\star(\mathfrak{q}) \geq \underline{u}_M\cos c > 0$ for all t implies (by the arguments in Isidori et al., 2003) that there exist ISS Lyapunov functions $V_\xi(\xi_1,\xi_2)$ and $V_\eta(\eta_1,\eta_2)$ *not dependent* on $\mathfrak{q}\in\Sigma$ for the dynamics (B.3) and (B.4). The small gain condition underlying the interconnection and the arguments in Mareels, Jiang, and Wang (1996) can be now used to claim the existence of a *locally Lipschitz* ISS Lyapunov function for the interconnection (B.3)–(B.4) and, in turn, for the overall lateral-longitudinal-vertical dynamics that is not dependent on $\mathfrak{q}$. Specifically, with n and $\zeta\in\mathbb{R}^n$ denoting respectively the dimension and the state of the overall closed-loop error system whose dynamics are compactly written as $\dot{\zeta} = f(\zeta,\delta_{FF},\mathfrak{q})$, there exist a locally Lipschitz Lyapunov function $V:\mathbb{R}^n\to\mathbb{R}$, class-$\mathcal{K}$ functions $\underline{\alpha}(\cdot), \overline{\alpha}(\cdot), \alpha(\cdot)$ and $\sigma(\cdot)$, positive M and Δ, *all independent of* $\mathfrak{q}$, such that for all $|\zeta|\leq M, |\delta_{FF}|\leq\Delta, \underline{\alpha}(|\zeta|)\leq V(\zeta)\leq\overline{\alpha}(|\zeta|)$, and for all $\mathfrak{q}\in\Sigma V^\circ(\zeta, f(\zeta,\delta_{FF},\mathfrak{q}))\leq -\alpha(|\zeta|)+\sigma(|\delta_{FF}|)$ where $V^\circ(\zeta,v)$ denotes the Clarke derivative of V at ζ along the direction v (see Clarke, 1990). Furthermore, there exists a constant $\bar{K} > 0$ such that $|(u_M(\sigma),u_F(\sigma))-(u_M^\star(\sigma),u_F^\star(\sigma))|\leq\bar{K}|\zeta|$ for all $\mathfrak{q}\in\Sigma$ and $|\zeta|\leq M$. From this the result of the proposition follows by standard ISS Lyapunov arguments with

$$\Delta_{FF,0} = \min\left\{\overline{\alpha}^{-1}\circ\underline{\alpha}\left(\frac{\mu}{1+\bar{K}}\right), \overline{\alpha}^{-1}\circ\underline{\alpha}(M)\right\}$$

$$\Delta_{FF,d} = \min\left\{\Delta, \overline{\sigma}^{-1}\circ\alpha\left(\frac{\mu}{1+\bar{K}}\right)\right\}.$$

Appendix C. Proof of Proposition 2 (sketch)

Let $\theta_1 := \tilde{\theta}, \theta_2 := \dot{\tilde{\theta}} + \frac{1}{K_D}\tilde{\theta}, \beta_1 := \tilde{\beta}, \beta_2 := \dot{\tilde{\beta}} + \frac{1}{K_D}\tilde{\beta}$. In these coordinates, system (9) controlled by (23) reads as the interconnection of

$$\begin{aligned}\dot{\theta}_1 &= -\frac{1}{K_D}\theta_1+\theta_2\\ \dot{\theta}_2 &= -K_PK_D\theta_2+\psi_\theta\left(\theta_1,\theta_2-\frac{1}{K_D}\theta_1,\beta_2-\frac{1}{K_D}\beta_1,\mathfrak{q}\right) \qquad \text{(C.1)}\\ &\quad-\frac{1}{K_D^2}\theta_1+\frac{1}{K_D}\theta_2+\delta_\theta(\mathfrak{q})\end{aligned}$$

and

$$\begin{aligned}\dot{\beta}_1 &= -\frac{1}{K_D}\beta_1+\beta_2\\ \dot{\beta}_2 &= -K_PK_D\beta_2+\psi_\beta\left(\theta_1,\theta_2-\frac{1}{K_D}\theta_1,\beta_2-\frac{1}{K_D}\beta_1,\mathfrak{q}\right) \qquad \text{(C.2)}\\ &\quad-\frac{1}{K_D^2}\beta_1+\frac{1}{K_D}\beta_2+\delta_\beta(\mathfrak{q})\end{aligned}$$

in which $\psi_\theta(\cdot)$ and $\Psi_\beta(\cdot)$ are properly defined locally Lipschitz functions such that $\psi_\theta(0,0,0,\mathfrak{q}) = \psi_\beta(0,0,0,\mathfrak{q}) = 0$ for all $\mathfrak{q}\in\Sigma$, and $\delta_{VI}(\mathfrak{q}) = \text{col}(\delta_\theta(\mathfrak{q}),\delta_\beta(\mathfrak{q}))$. Let $\rho := \max_{\mathfrak{q}\in\Sigma}\{\min\{\gamma_V^M,\gamma_V^F\}-|\theta^\star(\mathfrak{q})|\}$ and note that $\rho > c_1 > 0$. Lyapunov arguments (using $V_\theta(\theta_1,\theta_2) := \theta_1^2/(\rho-|\theta_1|)+\theta_2^2$, $V_\beta(\beta_1,\beta_2) := \beta_1^2+\beta_2^2$), show that for any $\Delta>0$ there exists a $K_P^\star>0$ such that for any $K_P\geq K_P^\star, \theta(t)\in(-\gamma_V^M,\gamma_V^F)$ for all $t\geq 0$ provided that $|\tilde{\theta}(0)|\leq c_1, |\dot{\tilde{\theta}}(0)|\leq c_2, |(\tilde{\beta}(0),\dot{\tilde{\beta}}(0))|\leq c_2$ and $|\delta_{VI}(\mathfrak{q})|\leq\Delta$, where c_2 is a positive number. The proof can be then completed by means of ISS and small gain arguments and by arguments that are similar to the ones used at the end of the proof of Proposition 1.

Appendix D. Proofs of Section 3.3

Proof of Proposition 3. The proof follows by joining the results of Propositions 1 and 2 and the definition of robust manoeuvres in Section 3.1. More specifically, note that if (25) holds then, by Proposition 1, it follows that $|(\xi(t),u(t))-(\xi_a^\star(\mathfrak{q}_a(t)),u_a^\star(\mathfrak{q}_a(t)))|\leq\mu$ for all t such that the vehicle is in free-flight. By the choice of $\mathfrak{q}_a(t)$ in item (a) and by definition of Σ_a' in the second relation of (14), it follows that $\mathcal{G}(FF,VI)$ is not intersected in the interval $[0,t_1']$ provided that $u(t) = u_{FF}(\mathfrak{q}_a(t))$, namely the vehicle evolves in free-flight in the time interval $[0,t_1']$. Furthermore, by definition of Σ_a'' in the third relation of (14), there exists a time $t_{s1}\leq t_1$ such that $(\xi(t_{s1}),u(t_{s1}))\in\mathcal{G}(FF,VI)$. This proves the first part of the proposition. Similar arguments can be adopted to prove the second part. In particular, note that if (26) holds, then, by Proposition 2, it follows that $|(\xi(t),u(t))-(\xi_b^\star(\mathfrak{q}_b(t)),u_b^\star(\mathfrak{q}_b(t)))|\leq\mu$ for all t such that the vehicle evolves in the VI mode. By this, the choice of $\mathfrak{q}_b(t)$ in item (b) and by definition of Σ_b' in the second relation of (15), it follows that the guard set $\mathcal{G}(VI,FF)$ is not intersected in the interval $[t_{s1},t_{s1}+t_2']$ provided that $u(t) = u_{VI}(\mathfrak{q}_b(t))$, namely the vehicle evolves robustly in the VI mode μ-close to the reference trajectory. Furthermore, by the definition of Σ_b'' in the third relation in (15), there exists a time $t_{s2}\leq t_{s1}+t_2$ such that $(\xi(t_{s2}),u(t_{s2}))\in\mathcal{G}(VI,FF)$. Finally, again by using Proposition 1 and the definition of Σ_c in (16), it turns out that that if $u = u_{FF}(\mathfrak{q}_c(t))$ then necessarily $\mathcal{G}(FF,VI)$ is not intersected and the vehicle evolves in free flight μ-close to the reference trajectory. □

Proof of Proposition 4. By integrating the dynamics (12) with initial condition $(\nu(t_{s1}),\dot{\nu}(t_{s1})) = (0,\dot{\alpha}_V(t_{s1}))$, $\dot{\alpha}_V(t_{s1})\geq 0$, and by considering $F_X(t)\equiv F_X(t_{s1})$ for all $t\in[t_{s1},t_{s1}+\delta T_i]$ (with δT_i denoting the impact interval), trivial bounds yield that if $(F_X(t_{s1})/M) > k_e^2\dot{\alpha}_V(t_{s1})^2/(4k_e-k_d)$ then necessarily $\nu(t)\geq 0$ for all $t\in[t_{s1},t_{s1}+\delta T_i]$. From this the result follows by using the definition of coefficient of restitution in Section 2.3. □

References

Aguiar, A. P., Hespanha, J. P., & Kokotovic, P. (2005). Path-following for non-minimum phase systems removes performance limitations. *IEEE Transactions on Automatic Control*, (2), 234–239.

Antonelli, G., Fossen, T. I., & Yoerger, D. (2008). Underwater robotics. In B. Siciliano, & O. Khatib (Eds.), *Springer handbook of robotics* (pp. 987–1008). Springer.

Brogliato, B. (1996). *Nonsmooth mechanics model, dynamics and control*. Springer.

Castillo, P., Lozano, R., & Dzul, A. E. (2003). *Modeling and control of mini flying machines*. Springer.

Clarke, F. H. (1990). *Optimization and non-smooth analysis*. SIAM Publishing.

Coelho, P., & Nunes, U. (2005). Path-following control of mobile robots in presence of uncertainties. *IEEE Transactions on Robotics*, (2), 252–261.

Egerstedt, Magnus (2000). Behavior based robotics using hybrid automata. In *HSCC* (pp. 103–116).

Feron, E., & Johnson, E. N. (2008). Aerial robotics. In B. Siciliano, & O. Khatib (Eds.), *Springer handbook of robotics*. Springer.

Frank, A., McGrew, J.S., Valenti, M., Levine, D., & How, J.P. (2007). Hover, transition, and level flight control design for a single-propeller indoor airplane. In *AIAA guidance, navigation and control conference. Hilton Head, USA* (pp. 3470–3475).

Frazzoli, E., Dahleh, M. A., & Feron, E. (2005). Maneuver-based motion planning for nonlinear systems with symmetries. *IEEE Transactions on Robotics*, *21*, 1077–1091.

Gavrilets, V. (2003). Aerobatic maneuvering of miniature helicopters. *Ph.D. thesis*. Massachussetts Institute of Technology.

Goebel, R., Sanfelice, R. G., & Teel, A. R. (2009). Hybrid dynamical systems. *IEEE Control Systems Magazine*, *29*, 28–93.

Goldsmith, W. (1960). *Impact*. London: Edward Arnold Publishers.

Hansen, J., Murray, J., & Campos, N. (2004). The NASA Dryden AAR project: a flight test approach to an aerial refueling system. In *AIAA atmospheric flight mechanics conference and exhibit*.

Harnoy, A., Friedland, B., & Cohn, S. (2008). Modeling and measuring friction effects. *IEEE Control System Magazine*, *28*(6), 82–91.

Hauser, J., Sastry, S., & Meyer, G. (1992). Nonlinear control design for slightly non-minimum phase systems: application to V/STOL aircraft. *Automatica*, *28*(4), 665–679.

Hughes, D. (2007). UAVs face hurdles in gaining access to civil airspace. Aviation week.

Isidori, A., Marconi, L., & Serrani, A. (2003). *Robust autonomous guidance*. Springer.

Johonson, E. N., & Turbe, M. A. (2005). Modeling, control and flight testing of a small ducted fan aircraft. In *AIAA guidance, navigation, and control conference and exhibit*.

Ko, A., Ohanian, O.J., & Gelhausen, P. (2007). Ducted fan UAV modeling and simulation in preliminary design. In *AIAA modeling and simulation technologies conference and exhibit*.

Lygeros, J., Johansson, K. H., Simić, S. N., Zhang, J., & Sastry, S. (2003). Dynamical properties of hybrid automata. *IEEE Transactions on Automatic Control*, *48*, 2–17.

Marconi, L., & Naldi, R. (2006). Nonlinear robust control of a reduced-complexity ducted MAV for trajectory tracking. In *44th IEEE CDC*.

Marconi, L., & Naldi, R. (2007). Robust nonlinear full degree of freedom control of an helicopter. *Automatica*, *42*, 1584–1596.

Mareels, I. M. Y., Jiang, Z. P., & Wang, Y. (1996). A Lyapunov formulation of the nonlinear small-gain theorem for interconnected ISS systems. *Automatica*, *32*, 1211–1215.

Matveev, A. S., & Savkin, A. V. (2000). *Qualitative theory of hybrid dynamical systems*. Birkhauser.

Naldi, R., Gentili, L., Marconi, L., & Sala, A. (2010). Design and experimental validation of a nonlinear control law for a ducted-fan miniature aerial vehicle. *Control Engineering Practice*, *18*(7), 747–760.

Nicholls, H. R., & Lee, M. H. (1989). A survey of robot tactile sensing technology. *The International Journal of Robotics Research*, *8*, 3–30.

Pflimlin, J.M., Binetti, P., Trouchet, D., Soueres, P., & Hamel, T. (2007). Aerodynamic modeling and practical attitude stabilization of a ducted fan UAV. In *Proceedings of the European control conference*.

Sanfelice, R. G., & Frazzoli, E. (2008). A hybrid control framework for robust maneuver-based motion planning. In *Proceedings of the 2008 American control conference*.

Scharf, D. P., Ploen, S. R., & Hadaegh, F. Y. A survey of spacecraft formation flying guidance and control (part I): guidance. In *2003 American control conference*.

Scherer, S., Singh, S., Chamberlain, L., & Saripalli, S. (2007). Flying fast and low among obstacles. In *IEEE international conference on robotics and automation*.

Skjetne, R., Fossen, T. I., & Kokotovic, P. (2004). Robust output maneuvering for a class of nonlinear systems. *Automatica*, (3), 373–383.

Stengel, R. F. (2004). *Flight dynamics*. Princeton University Press.

Sullivan, J. M. (2006). Evolution or revolution? the rise of UAVs. *IEEE Technology and Society Magazine*, *25*(3), 43–49. Fall.

Tavernini, L. (1987). Differential automata and their discrete simulators. *Nonlinear Analysis: Theory, Methods & Applications*, *11*, 665–683.

Theodore, C., Sheldon, S., Rowley, D., McLain, T., Dai, W., & Takahashi, M. (2005). Full mission simulation of a rotorcraft unmanned aerial vehicle for landing in a non-cooperative environment. In *61st annual forum of the American helicopter society*.

Lorenzo Marconi graduated in 1995 in Electrical Engineering from the University of Bologna. Since 1995 he has been with the Department of Electronics, Computer Science and Systems at University of Bologna, where he obtained his Ph.D. degree in March 1998. From 1999 he has been an Assistant Professor in the same Department where he is now Associate Professor since January 2005. He has held visiting positions at various international academic/research institutions. He is co-author of more than 100 technical publications on the subject of linear and nonlinear feedback design published on international journals, books and conference proceedings. In 2005, he received the "Outstanding Application Paper Award" from the International Federation of Automatic Control (IFAC) for a co-authored paper published on *Automatica*. He is member of the IEEE Control System Society, of the Control System Society Conference Editorial Board and of IFAC Technical Committees on "Nonlinear Control Systems" and "Safety and Supervision in Technical Processes". His current research interests include nonlinear control, output regulation, control of autonomous vehicles, fault detection and isolation, fault tolerant control.

Roberto Naldi graduated in 2004 in Computer Science Engineering from the University of Bologna. Since 2004 he has been with the Department of Electronics, Computer Science and Systems at University of Bologna, where he obtained his Ph.D. degree in May 2008. His main research interest is control of unmanned aerial vehicles.

Luca Gentili graduated in Electronic Engineering at the University of Bologna in 2000; he obtained his Ph.D. at the University of Bologna in 2004. From 2004 to 2010 he held a Post-doc position at the Department of Electronics, Computer Sciences and Systems at the University of Bologna working on industrial automation, aerial robotics, modelling, dynamic simulations and nonlinear control. From 2010 he is Development Engineer at Tetra Pak Packaging Solutions S.p.A.